

Diacylglycerol-mediated regulation of *Aplysia* bag cell neuron excitability requires protein kinase C

Raymond M. Sturgeon and Neil S. Magoski

Department of Biomedical and Molecular Sciences, Physiology Graduate Program, Queen's University, Kingston, ON, Canada, K7L 3N6

Key points

- In *Aplysia*, reproduction is initiated by the bag cell neurons and a prolonged period of enhanced excitability known as the afterdischarge.
- Phosphoinositide turnover is upregulated during the afterdischarge resulting in the hydrolysis of phosphatidylinositol-4,5-bisphosphate by phospholipase C (PLC) and the release of diacylglycerol (DAG) and inositol trisphosphate (IP₃).
- In whole-cell voltage-clamped cultured bag cell neurons, 1-oleoyl-2-acetyl-*sn*-glycerol (OAG), a synthetic DAG analogue, activates a dose-dependent, transient, inward current (I_{OAG}) that is enhanced by IP₃, mimicked by PLC activation and dependent on basal protein kinase C (PKC) activity.
- OAG depolarizes bag cell neurons and triggers action potential firing in culture, and prolongs electrically stimulated afterdischarges in intact bag cell neuron clusters *ex vivo*.
- Although PKC alone cannot activate the current, it is required for I_{OAG} ; this is the first description of required obligate PKC activity working in concert with PLC, DAG and IP₃ to maintain the depolarization required for prolonged excitability in *Aplysia* reproduction.

Abstract Following synaptic input, the bag cell neurons of *Aplysia* undergo a long-term afterdischarge of action potentials to secrete egg-laying hormone and initiate reproduction. Early in the afterdischarge, phospholipase C (PLC) hydrolyses phosphatidylinositol-4,5-bisphosphate into inositol trisphosphate (IP₃) and diacylglycerol (DAG). In *Aplysia*, little is known about the action of DAG, or any interaction with IP₃; thus, we examined the effects of a synthetic DAG analogue, 1-oleoyl-2-acetyl-*sn*-glycerol (OAG), on whole-cell voltage-clamped cultured bag cell neurons. OAG induced a large, prolonged, Ca²⁺-permeable, concentration-dependent inward current (I_{OAG}) that reversed at ~ -20 mV and was enhanced by intracellular IP₃. A similar current was evoked by either another DAG analogue, 1,2-dioctanoyl-*sn*-glycerol (DOG), or activating PLC with *N*-(3-trifluoromethylphenyl)-2,4,6-trimethylbenzenesulfonamide (*m*-3M3FBS). I_{OAG} was reduced by the general cation channel blockers Gd³⁺ or flufenamic acid. Work in other systems indicated that OAG activates channels independently of protein kinase C (PKC); however, we found pretreating bag cell neurons with any of the PKC inhibitors bisindolylmaleimide, sphinganine, or H7, attenuated I_{OAG} . However, stimulating PKC with phorbol 12-myristate 13-acetate (PMA) did not evoke current or enhance I_{OAG} ; moreover, unlike PMA, OAG failed to trigger PKC, as confirmed by an independent bioassay. Finally, OAG or *m*-3M3FBS depolarized cultured neurons, and while OAG did not provoke afterdischarges from bag cell neurons in the nervous system, it did double the duration of synaptically elicited afterdischarges. To our knowledge, this is the first report of obligate PKC activity for I_{OAG} gating. An interaction between phosphoinositol metabolites and PKC could control the cation channel to influence afterdischarge duration.

(Received 13 January 2016; accepted after revision 17 May 2016; first published online 20 May 2016)

Corresponding author N. S. Magoski: Queen's University, Department of Biomedical and Molecular Sciences, 4th Floor, Botterell Hall, 18 Stuart Street, Kingston, ON, Canada, K7L 3N6. Email: magoski@queensu.ca

Abbreviations Bis, bisindolylmaleimide I; $[Ca^{2+}]_i$, intracellular Ca^{2+} ; DAG, diacylglycerol; DOG, 1,2-dioctanoyl-*sn*-glycerol; ELH, egg-laying hormone; FFA, flufenamic acid; IP₃, inositol trisphosphate; KW, Kruskal–Wallis; *m*-3M3FBS, *N*-(3-trifluoromethylphenyl)-2,4,6-trimethylbenzenesulfonamide; nASW, normal artificial sea water; *o*-3M3FBS, *N*-(2-trifluoromethylphenyl)-2,4,6-trimethylbenzenesulfonamide; OAG, 1-oleoyl-2-acetyl-*sn*-glycerol; PIP₂, phosphatidylinositol 4,5-bisphosphate; PKC, protein kinase C; PLC, phospholipase C; PMA, phorbol 12-myristate 13-acetate; 9-Pt, 9-phenanthrol; SAG, 1-stearoyl-2-arachidonoyl-*sn*-glycerol; sphinganine, D-erythro-dihydrosphingosine; tcASW, tissue culture artificial sea water; TRP, transient receptor potential; V_{REV} , reversal potential.

Introduction

The inositol lipid pathway is essential in converting extracellular signals to intracellular mediators (Fisher *et al.* 2002; Berridge, 2009; Fukami *et al.* 2010). Hydrolysis of phosphatidylinositol 4,5-bisphosphate (PIP₂) by phospholipase C (PLC) simultaneously generates two important second messengers: inositol trisphosphate (IP₃) and diacylglycerol (DAG) (Berridge & Irvine, 1989; Rhee, 2001). Since the discovery of phosphoinositide turnover, much emphasis has been on IP₃ and intracellular Ca^{2+} ($[Ca^{2+}]_i$) mobilization (Michell, 1975; Berridge & Irvine, 1984; Perney & Kaczmarek, 1992; Savolainen *et al.* 1994; Decrock *et al.* 2013). On the other hand, DAG has been defined as a protein kinase C (PKC) activator (Takai *et al.* 1979; Kishimoto *et al.* 1980; Nishizuka, 1988); in addition, DAG and its synthetic analogues can directly open certain transient receptor potential (TRP) channels (Hofmann *et al.* 1999; Okada *et al.* 1999; Venkatachalam *et al.* 2003), or evoke inward currents in various tissues (Helliwell & Large, 1997; Albert & Large, 2003; Bandyopadhyay & Payne, 2004; Tu *et al.* 2009). However, contrasting reports indicate that the DAG analogue, OAG, fails to produce inward currents in rat pontine neurons (Li *et al.* 1999), while actually inhibiting Na⁺, K⁺, or Ca²⁺ currents in hippocampal and sensory neurons (Rane & Dunlap, 1986; Doerner *et al.* 1988; Cantrell *et al.* 1996).

In the marine mollusc *Aplysia californica*, a group of neuroendocrine cells known as the bag cell neurons are responsible for initiating reproduction, and provide a tractable system for studying ion channel modulation (Conn & Kaczmarek, 1989; Zhang *et al.* 2008). In response to cholinergic synaptic input, the bag cell neurons enter a period of enhanced excitability, known as the afterdischarge (Kupfermann & Kandel, 1970; White & Magoski, 2012). This synchronous burst of action potentials starts with a fast phase of 5 Hz firing for ~1 min, followed by a 1 Hz slow phase of ~30 min, and culminates in the release of egg-laying hormone (ELH) (Arch, 1972; Loechner *et al.* 1990; Michel & Wayne, 2002). During the slow phase of the afterdischarge, PLC-mediated phosphoinositide turnover leads to an elevation of PKC activity and IP₃ levels (Fink *et al.* 1988). In bag cell and other *Aplysia* neurons, there are reports examining the effect of PLC (Fulton *et al.* 2008), and the role of IP₃ liberating Ca²⁺ (Fink *et al.* 1988; Sawada *et al.* 1989) or modulating cation channels

(Gardam & Magoski, 2009). However, there is currently no information about the effects of DAG in this system.

Here, using cultured bag cell neurons, we examine the effects of the synthetic DAG analogue, 1-oleoyl-2-acetyl-*sn*-glycerol (OAG), as well as pharmacological activation of PLC, and show that both treatments evoke a similar inward, cationic current. Moreover, we establish that, unlike other examples for OAG-gated currents, basal PKC activity is required to apparently prime the current, but PKC alone does not actively elicit the response, suggesting a synergy of PLC pathway signalling molecules and effectors is necessary for channel opening. These results are consistent with PKC being turned on to maintain the afterdischarge and thereby trigger hormone secretion and reproduction.

Methods

Animals and cell culture

Adult *Aplysia californica* (a hermaphrodite) weighing 200–650 g were obtained from Marinus (Long Beach, CA, USA). They were housed in an ~300 litre aquarium containing continuously circulating, aerated sea water (Instant Ocean; Aquarium Systems, Mentor, OH, USA) at 14–16°C on a 12 h:12 h light–dark cycle and fed romaine lettuce five times per week. All experiments were approved by the Queen's University Animal Care Committee (protocols Magoski-100323 or Magoski-100845).

For primary cultures of isolated bag cell neurons, animals were anaesthetized by an injection of isotonic MgCl₂ (~50% of body weight) and the abdominal ganglion was removed and treated with dispase II (13.3 mg ml⁻¹; no. 165859; Roche Diagnostics, Indianapolis, IN, USA) dissolved in tissue culture artificial sea water (tcASW) (composition in mM: 460 NaCl, 10.4 KCl, 11 CaCl₂, 55 MgCl₂, 15 HEPES, 1 mg ml⁻¹ glucose, 100 U ml⁻¹ penicillin, and 0.1 mg ml⁻¹ streptomycin; pH 7.8 with NaOH) for 18 h at 22°C. The ganglion was then rinsed in tcASW for 1 h, and the bag cell neuron clusters were dissected from their surrounding connective tissue. With the use of a fire-polished glass Pasteur pipette and gentle trituration, neurons were dissociated and dispersed in tcASW onto 35 mm × 10 mm polystyrene tissue culture dishes (BD Falcon; Becton-Dickinson,

Franklin Lakes, NJ, USA). Cultures were maintained in a 14°C incubator in tcASW and used for experimentation within 1–3 days. Salts were obtained from Fisher Scientific (Ottawa, ON, Canada), MP Biomedicals (Aurora, OH, USA) or Sigma-Aldrich (Oakville, ON, Canada).

Whole-cell voltage-clamp and sharp-electrode current-clamp recording from cultured bag cell neurons

Voltage-clamp recordings of membrane current from cultured bag cell neurons were performed at room temperature (20–22°C) using an EPC 8 amplifier (HEKA Elektronik, Harvard Apparatus Canada, Saint-Laurent, QC, Canada) and the tight-seal, whole-cell method (Hamill *et al.* 1981). Microelectrodes were pulled from 1.5 mm/1.12 mm external/internal diameter, borosilicate glass capillaries (TW150F-4; World Precision Instruments, Sarasota, FL, USA) and had a resistance of 1–2 MΩ when filled with intracellular saline (see below). Pipette junction potentials were nulled immediately before seal formation; after making a seal, pipette capacitive currents were cancelled. Following membrane rupture, neuronal capacitive currents were cancelled and the series resistance (3–5 MΩ) was compensated to 70–80% and monitored throughout the experiment. Current was filtered at 1 kHz with the EPC 8 Bessel filter and sampled at 2 kHz using a Digidata 1322A analog-to-digital converter (Molecular Devices, Sunnyvale, CA, USA), the Clampex acquisition program of pCLAMP v10.0 (Molecular Devices), and an IBM-compatible personal computer.

Unless otherwise noted, most recordings were made in normal artificial sea water (nASW; composition as per tcASW but lacking glucose and antibiotics) with Cs⁺-based intracellular saline (composition in mM: 500 caesium aspartate, 70 CsCl, 1.25 MgCl₂, 10 Hepes, 11 glucose, 10 glutathione, 5 EGTA, 5 adenosine 5′-triphosphate 2Na·H₂O (Sigma-Aldrich) and 0.1 guanosine 5′-triphosphate Na·H₂O (Sigma-Aldrich); pH 7.3 with KOH). The free Ca²⁺ concentration was set at 300 nM by adding 3.32 mM CaCl₂, as calculated using WebMaxC (<http://web.stanford.edu/~cpatton/webmaxc.htm>). A junction potential of 17 mV was calculated for the intracellular saline vs. nASW and compensated for by subtraction off-line.

In one set of experiments, rapid, voltage-gated Ca²⁺ currents were recorded using Ca²⁺-Cs⁺-TEA-ASW, where Na⁺ was replaced with tetraethylammonium (TEA) and K⁺ with Cs⁺ (composition in mM: 460 TEA-Cl, 10.4 CsCl, 55 MgCl₂, 11 CaCl₂, and 15 Hepes; pH 7.8 with CsOH). In this case, the same Cs⁺-based internal saline, but with no added Ca²⁺, was used. On-line leak subtraction involved a P/4 protocol from –60 mV with subpulses of opposite polarity and one-quarter the magnitude, an inter-subpulse interval of 500 ms, and 100 ms before actual test pulses

of 200 ms (see Results for details). A junction potential of 20 mV was subtracted off-line.

Current-clamp recordings were made from cultured bag cell neurons in nASW using an AxoClamp 2B (Molecular Devices) amplifier and the sharp-electrode, bridge-balanced method. Microelectrodes were pulled from 1.2 mm/0.9 mm external/internal diameter borosilicate glass capillaries (TW120F-4; World Precision Instruments) and had a resistance of 8–35 MΩ when filled with 2 M potassium acetate plus 10 mM Hepes and 100 mM KCl (pH 7.3 with KOH). To balance the bridge, current pulses were delivered with a Grass S88 stimulator (Astro-Med, Longueuil, QC, Canada); in addition, neurons were manually set to –60 mV in current clamp by delivering constant bias current with the AxoClamp DC current command. Voltage was filtered at 3 kHz using the Axoclamp Bessel filter and sampled at 2 kHz as per voltage clamp.

Ca²⁺ imaging

Ca²⁺ imaging was performed under whole-cell voltage clamp, during which the intracellular saline was supplemented with 1 mM fura-PE3 (Teflabs, Austin, TX, USA) to dye-fill neurons via passive dialysis, as previously done in our laboratory (Geiger *et al.* 2009; Groten *et al.* 2013; Groten & Magoski, 2015). Imaging was performed using a TS100-F inverted microscope (Nikon, Mississauga, ON, Canada) equipped with a Nikon Plan Fluor ×20 objective (NA = 0.5). The light source was a 75 W Xe arc lamp and a multi-wavelength DeltaRAM V monochromatic illuminator (Photon Technology International, London, ON, Canada) coupled to the microscope with a UV-grade liquid light guide. Excitation wavelengths were 340 and 380 nm. Between acquisition episodes, the excitation illumination was blocked by a shutter, which, along with the excitation wavelength, was controlled by an IBM-compatible computer, a Photon Technology International computer interface, and EasyRatio Pro software v1.10 (Photon Technology International). Emitted light passed through a 400 nm long-pass dichroic mirror and a 510 nm/40 nm emission barrier filter before being detected by a Photometrics (Tucson, AZ, USA) CoolSNAP HQ² charge-coupled device camera. Camera gain was maximized and exposure time was 1 s during both 340 and 380 nm excitation. Background was removed by setting a minimal threshold value of 300 arbitrary units of fluorescence. Fluorescence signals were acquired using regions of interest positioned over neuronal somata, at approximately the midpoint of the vertical focal plane and one-half to three-quarters of the cell diameter, and then averaged eight frames per acquisition. The total acquisition time permitted a sampling rate of 0.5 Hz for both wavelengths altogether. The ratio of the emission following 340 and 380 nm excitation (340/380) was taken

to reflect free $[Ca^{2+}]_i$ (Grynkiewicz *et al.* 1985) and saved for subsequent analysis. Image acquisition, emitted light sampling, and ratio calculations were performed using EasyRatio Pro.

Ensemble extracellular and single-neuron sharp-electrode current-clamp recording from the intact bag cell neuron cluster

For extracellular recording, the abdominal ganglion was maintained in a nASW-filled dish kept at a 14°C by immersion in a water-cooled chamber. A wide-bore, fire-polished glass suction recording electrode (containing nASW) was placed over one of the two bag cell neuron clusters, while a similar stimulating electrode was placed at the rostral end of the ipsilateral pleuroabdominal connective corresponding to the recorded cluster. Stimulating current pulses were delivered with a Grass SD9 stimulator while voltage was monitored with a Model 3000 AC/DC differential amplifier (A-M Systems; Sequim, WA, USA). Voltage was high-pass filtered at 10 Hz and low-pass filtered at 1 kHz using the amplifier cutoff filters, and acquired at a sampling rate of 2 kHz using Axoscope v9.0 (Molecular Devices) as per voltage clamp.

Intracellular recording from single bag cell neurons in the intact cluster employed the sharp-electrode, bridge-balanced method, but in this case with the use of a Neuroprobe 1600 amplifier (A-M Systems). To facilitate sharp-electrode impalement, ganglia were treated with 0.5 mg ml⁻¹ elastase (E1250; Sigma-Aldrich) and 1 mg ml⁻¹ collagenase/dispase (Roche Diagnostics) for 2.5 h (Kehoe, 1972; Fisher *et al.* 1994), and then the cluster contralateral from the extracellular electrode was desheathed using fine forceps. Voltage was filtered at 1 kHz using the Neuroprobe Bessel filter and acquired with Axoscope at 2 kHz.

Drug application and reagents

All solution exchanges were accomplished using a calibrated transfer pipette to replace the bath (culture dish) tcASW with the desired extracellular saline. Drugs were introduced by initially removing a small volume (~30 µl) of saline from the bath, combining that with an even smaller volume (<10 µl) of drug stock solution and then reintroducing that mixture back into the bath. Care was taken to pipette near the side of the dish and as far away as possible from the neurons. For a small number of specific experiments, acetylcholine was pressure ejected from an unpolished patch pipette (1–2 µm bore) for 2 s at 75–150 kPa using a PMI-100 pressure microinjector (Dagan, Minneapolis, MN, USA), as done previously by our lab (White & Magoski, 2012; White *et al.* 2014) and others (Fisher *et al.* 1993). The pipette was removed from

the bath immediately after each ejection to minimize leakage and possible desensitization.

All drugs were made up as stock solutions in dimethyl sulfoxide (DMSO; Fisher) or H₂O and frozen at –20°C, then diluted down to a working concentration daily as needed. 1-oleoyl-2-acetyl-*sn*-glycerol (OAG; Sigma-Aldrich), 1,2-dioctanoyl-*sn*-glycerol (DAG; Cayman Chemical, Ann Arbor, MI, USA), 9-phenanthrol (9-PT; Sigma-Aldrich), bisindolylmaleimide I (Bis; EMD Millipore, Etobicoke, ON, Canada), D-erythro-dihydro-sphingosine (sphinganine; Sigma-Aldrich), flufenamic acid (FFA; Sigma-Aldrich), *N*-(3-trifluoromethylphenyl)-2,4,6-trimethylbenzenesulfonamide (*m*-3M3FBS; Sigma-Aldrich), *N*-(2-trifluoromethylphenyl)-2,4,6-trimethylbenzenesulfonamide (*o*-3M3FBS; Tocris Bioscience, Bristol, UK), and phorbol 12-myristate 13-acetate (PMA; Sigma-Aldrich) were dissolved in DMSO. DOG and 1-stearoyl-2-arachidonoyl-*sn*-glycerol (SAG; Cayman) were dried under N₂ to remove solvent, and the lipids were resuspended in DMSO and ethanol, respectively. The maximal final concentrations of DMSO or ethanol ranged from 0.05 to 0.4% (v/v), which in control experiments both here and in previous work from our laboratory had no effect on holding current, membrane conductance, fura PE3 fluorescence, or membrane potential (Tam *et al.* 2011; Groten *et al.* 2013; Hickey *et al.* 2013; Dargaei *et al.* 2014, 2015). Acetylcholine chloride (Sigma-Aldrich), D-*myo*-inositol 1,4,5-trisphosphate trisodium salt (IP₃; Sigma-Aldrich), gadolinium(III) chloride hexahydrate (Gd³⁺; Sigma-Aldrich), and H-7 dihydrochloride (H7; Tocris) were dissolved in H₂O.

Analysis

The Clampfit analysis program of pCLAMP was used to determine the amplitude of changes to holding current or membrane potential evoked by drugs under voltage- or current-clamp. For area calculation, two cursors were placed 30 s apart immediately prior to drug addition, the average of which served as a baseline. An additional two cursors were placed at the first indication of current response and 15 min later, respectively. Clampfit then calculated the area above the current relative to the established pre-drug baseline. For determining the amplitude of sharp peaks in I_{OAG} , a cursor was placed at the base of the peak, immediately prior to the large increase in inward current, and a second cursor was placed at the top of the peak; the amplitude was taken as the difference in the current between the top (nadir) of the inward peak and the level prior to the peak. For current-clamp recordings, Clampfit was used to generate all-points histograms for before and after drug addition. Using Clampfit, the largest peak of the resulting histograms was fitted with a Gaussian function by the least-squares method using a simplex

search, and taken as the average membrane potential. For display only, some of the current traces were filtered off-line to between 20 and 80 Hz using the Clampfit Gaussian filter. Due to the overall slow nature of the current responses, the second filtering brought about no change in amplitude or kinetics. Conductance was derived using Ohm's law ($G = I/V$) and the current change during a 200 ms step from -60 to -70 mV. Reversal potential (V_{REV}) was determined from a ramp protocol (see Results for details); specifically, two cursors were placed ~ 250 ms on either side of the point where the current appeared to cross the Y -axis and this region was fitted with a straight line equation ($y = mx + b$), where m was the slope and b was the Y -intercept, the latter being taken as V_{REV} .

For $[Ca^{2+}]_i$, EasyRatio Pro files were exported as .txt files and plotted as line graphs using Prism v5.04 (GraphPad Software, Inc., La Jolla, CA, USA). Analysis compared the steady-state value of the baseline 340/380 ratio with the ratio from a peak or new steady state during OAG application. Averages of the baseline and new regions were determined by eye, if an obvious change in the ratio corresponded to a peak in the simultaneous holding current recording. Change was the difference between the new and the baseline ratio.

The current–voltage relationship of Ca^{2+} currents was established using Clampfit. Following leak subtraction (see 'Whole-cell voltage-clamp and sharp-electrode current-clamp recording from cultured bag cell neurons' for details) to set the baseline at 0 nA, an initial cursor was placed immediately following the artifact from the voltage step, and another cursor was placed 100 ms after that. The negative peak current between these two cursors was taken as the rapid Ca^{2+} current elicited by the step. Current was normalized to cell size by dividing by the whole-cell capacitance (as provided by the EPC 8 slow capacitance compensation circuitry) and plotted against step voltage in Prism.

Data are means \pm standard error of the mean. Statistical analysis was performed using InStat v3.10 (GraphPad Software). The Kolmogorov–Smirnov method was used to test data sets for normality. To test whether the mean differed between two groups, either Student's paired or unpaired t test (for normally distributed data) with Welch correction as necessary, or the Mann–Whitney U test (for not normally distributed data), was used. For three or more means, normally distributed data were compared using a standard one-way analysis of variance (ANOVA) followed by the Student–Newman–Keuls test, whereas not normally distributed data were compared using the Kruskal–Wallis (KW) ANOVA and Dunn's multiple comparisons test. Means were considered significantly different if the two-tailed P value was <0.05 .

Results

A DAG analogue activates a prolonged inward current in cultured bag cell neurons

OAG, a DAG analogue, has been shown to activate the non-selective cation channels TRPC3 and TRPC6 (Hofmann *et al.* 1999; Okada *et al.* 1999; Venkatachalam *et al.* 2003), and an endogenous inward current through a PKC-independent mechanism (Albert & Large, 2003), but the effects of OAG on *Aplysia* neurons, and possible DAG-dependent effects during the afterdischarge, are largely unknown. As such, we examined the effects of OAG on whole-cell currents of bag cell neurons in primary culture, using a Cs^+ -Asp-based intracellular solution and a nASW external solution, with the area above the current as quantification.

Compared to DMSO (the vehicle) (Fig. 1A), bath application of OAG to bag cell neurons voltage-clamped at -60 mV resulted in a large, transient inward current (hereafter referred to as I_{OAG}) that was dose-dependent between 1 and 100 μM (Fig. 1B). Following OAG delivery, at the first sign of a change in the holding current, the area above the current was measured for a 15 min period following onset (see Methods for details). Previous reports used a range of OAG concentrations from 3 to 100 μM (Strong *et al.* 1987a; Helliwell & Large, 1997; Hofmann *et al.* 1999; Albert & Large, 2003), and we opted for 25 μM , which evoked a significant and reproducible effect ($n = 8$). At this concentration, I_{OAG} presented with a variable latency (91 ± 18.9 s; $n = 6$), was often punctuated with large, transient, sharp peaks (average of -3.8 ± 0.9 nA; $n = 6$) (see Methods for details on calculating peak amplitude), and returned to a steady holding current of ~ 1 nA (Fig. 1B, upper-middle). A similar increase in current with subsequent recovery in the continued presence of OAG has been reported for both macroscopic and single channels in myocytes and cell lines (Helliwell & Large, 1997; Hofmann *et al.* 1999; Albert & Large, 2003).

Delivery of 100 μM OAG ($n = 5$) resulted in a marked increase in current, as well as the number of sharp peaks observed and the mean amplitude of these peaks (-5.47 ± 1.7 nA, $n = 5$) (Fig. 1B, lower). The greater quantity of current peaks and overall more noisy response with 100 μM OAG may have contributed to the enhanced variability and concomitant large standard error for the average data at this higher concentration (Fig. 1C). Conversely, at 1 μM OAG ($n = 2$) there was no clear change in holding current, similar to DMSO (Fig. 1B, upper, and C). For DMSO and other recordings that did not show an obvious current, the starting point for the area above the current calculation was a time point approximately equal to the mean latency of I_{OAG} ,

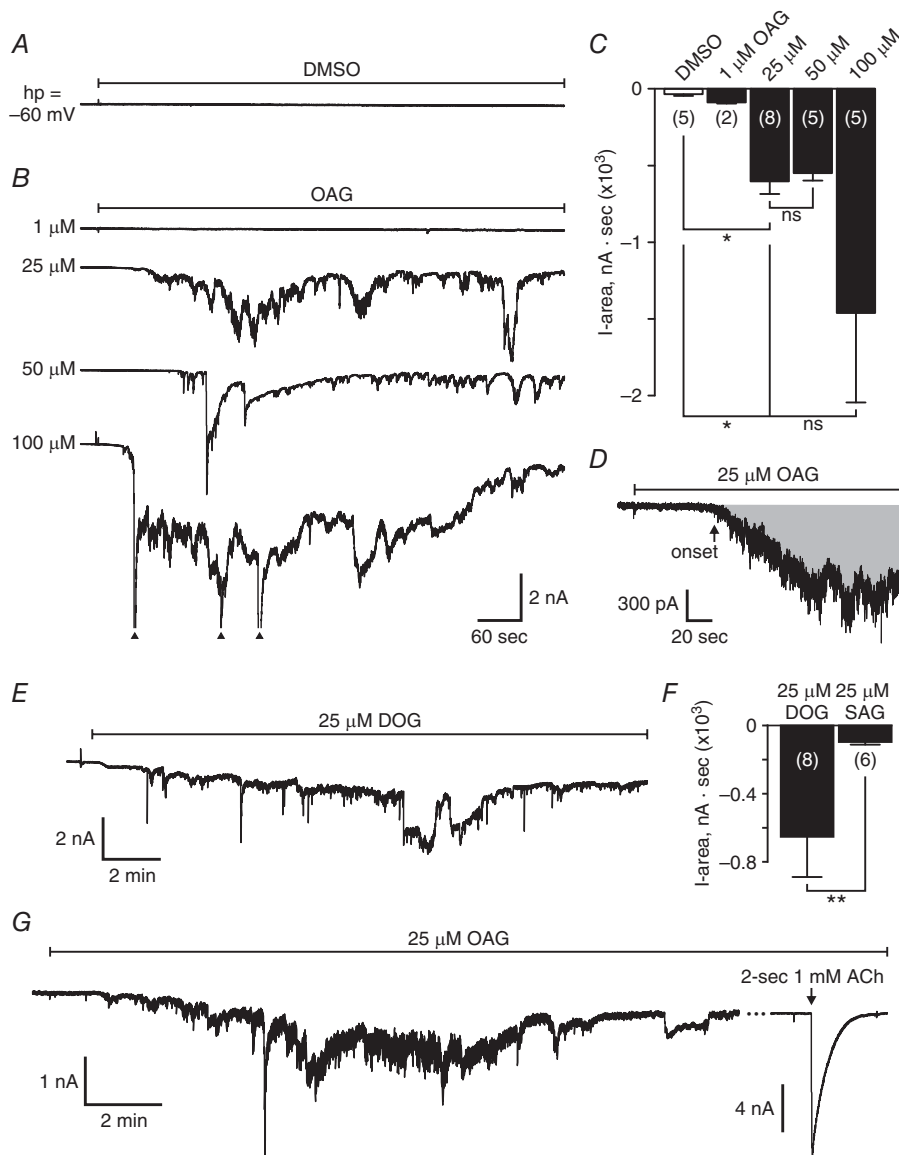


Figure 1. The DAG analogue OAG evokes an inward current in cultured bag cell neurons

Neurons are whole-cell voltage-clamped at a holding potential (hp) of -60 mV in nASW using Cs^+ -Asp-based intracellular solution. *A*, bath application of the vehicle, 0.1% (v/v) DMSO (at bar), elicits no obvious current. *B*, when OAG is delivered at the concentrations indicated, a noisy current is apparent starting at $25 \mu\text{M}$. Each recording is from a separate neuron. Scale bars apply to all traces in *A* and *B*. Arrowheads indicate truncation of current responses that briefly exceeded the gain of the amplifier. *C*, summary concentration-response graph presented as area above the induced current. There is essentially no change in current following DMSO (-34.9 ± 10.8 nA · s) or $1 \mu\text{M}$ OAG (-88.1 ± 7.4 nA · s). Higher OAG concentrations result in currents that are significantly larger than control: $25 \mu\text{M} = -602.9 \pm 82.9$; $50 \mu\text{M} = -549.2 \pm 49.2$; $100 \mu\text{M} = -1462.1 \pm 583.3$ (all quantified as nA · s) ($P = 0.0087$, KW ANOVA; $*P < 0.05$, Dunn's multiple comparisons test; ns: not significant). For this and all subsequent bar graphs, the n value is indicated within, just above or below, the individual bar, and error bars reflect the standard error of the mean. *D*, example of I_{OAG} onset at $25 \mu\text{M}$ OAG. Baseline for area calculation is the mean of a 30 s period prior to the addition of OAG; the area of I_{OAG} (shaded) is calculated for a 15 min period following onset, although most traces in this and other figures show 13.5 min, comprising 30 s before OAG addition, ~ 2 – 3 min latency and 10 min of current. Latency of I_{OAG} varies between trials; therefore, onset is taken as the first clear change in current after OAG addition. *E*, bath application of $25 \mu\text{M}$ DOG, another membrane-permeable DAG analogue, induces a similar effect to I_{OAG} . *F*, summary data of the area above the current for DOG and SAG, a membrane-impermeable DAG analogue (DOG = -652.6 ± 236.2 nA · s; SAG = -96.5 ± 15.3 nA · s) ($**P = 0.0027$, Mann-Whitney unpaired U test). *G*, a 2 s pressure application of 1 mM acetylcholine (ACh) (right) to a bag cell neuron following current induced by $25 \mu\text{M}$ OAG (left) shows the neurons are still acetylcholine-responsive. The recording is separated, at ellipsis, and the scale of the ordinate different between left and right for display purposes. Time base at left applies to both traces.

i.e. 90 s. See Fig. 1D for an example of a point in a recording chosen as onset, as well as latency of I_{OAG} . In addition, we investigated a second membrane-permeable DAG analogue, 1,2-dioctanoyl-*sn*-glycerol (DOG), as well as a membrane-impermeable DAG analogue, 1-stearoyl-2-arachidonoyl-*sn*-glycerol (SAG), for the possibility of evoking current. Bath application of $25 \mu\text{M}$ DOG to cultured bag cell neurons produced a current similar to I_{OAG} (Fig. 1E). The current elicited by DOG began with a smooth transition, followed by large and more noisy deflections similar to I_{OAG} . SAG failed to evoke a response. The area of the DOG-induced current was similar to I_{OAG} , at $\sim 600 \text{ nA} \cdot \text{s}$, although the effect was significantly larger than any current produced by SAG (Fig. 1F).

The noisy nature of I_{OAG} prompted us to confirm that the neurons retained the ability to subsequently respond to other stimuli. As an assay of cell viability, we used a pressure-application of acetylcholine (see Methods for details). Previous work in our lab has indicated that cultured bag cell neurons exhibit a large inward current in response to acetylcholine, which appears to be a key trigger to stimulate the afterdischarge in the intact cluster (White & Magoski, 2012). After I_{OAG} had returned to baseline, a 2 s pressure-application of 1 mM acetylcholine caused a large inward current followed by a prompt recovery (Fig. 1G). In the neurons tested with acetylcholine post-OAG, the mean capacitance-normalized peak response was $-44.2 \pm 10.6 \text{ nA nF}^{-1}$ ($n = 5$). We also used a second acetylcholine pressure-ejection to examine the remaining current as a reflection of receptor desensitization. For these same neurons, when acetylcholine was applied a second time, the subsequent acetylcholine response was $77.7 \pm 6.3\%$ ($n = 5$) in magnitude of the initial current (data not shown).

I_{OAG} increases membrane conductance in a manner consistent with opening of a non-selective cation channel

To examine conductance and reversal potential during I_{OAG} , cultured bag cell neurons were again voltage-clamped at -60 mV in nASW with Cs^+ -Asp-based intracellular saline. A 200 ms pulse to -70 mV was delivered, followed by a 5 s ramp from -80 to 0 mV , before and after bath application of $25 \mu\text{M}$ OAG (Fig. 2A). The change in membrane conductance was calculated as a percentage change in the current produced by the step to -70 mV (Fig. 2B), as per our investigations of other currents in bag cell neurons (Hung & Magoski, 2007; Gardam *et al.* 2008; Hickey *et al.* 2010; White & Magoski, 2012). There was an $\sim 200\%$ increase in the current during the step at peak I_{OAG} vs. the step immediately prior to OAG ($n = 8$) (Fig. 2B, left). Compared to DMSO, which elevated the conductance by only 35% ($n = 7$), the change after the

delivery of OAG was significant, consistent with channel opening during I_{OAG} (Fig. 2B, right).

Reversal potential (V_{REV}) was derived from the ramp difference current, i.e. the current evoked by the ramp before OAG, subtracted from current evoked by the ramp at peak I_{OAG} . The difference current was essentially linear, showed no obvious voltage dependence and presented a V_{REV} of $-22.5 \pm 2.1 \text{ mV}$ for I_{OAG} ($n = 7$) (Fig. 2C,

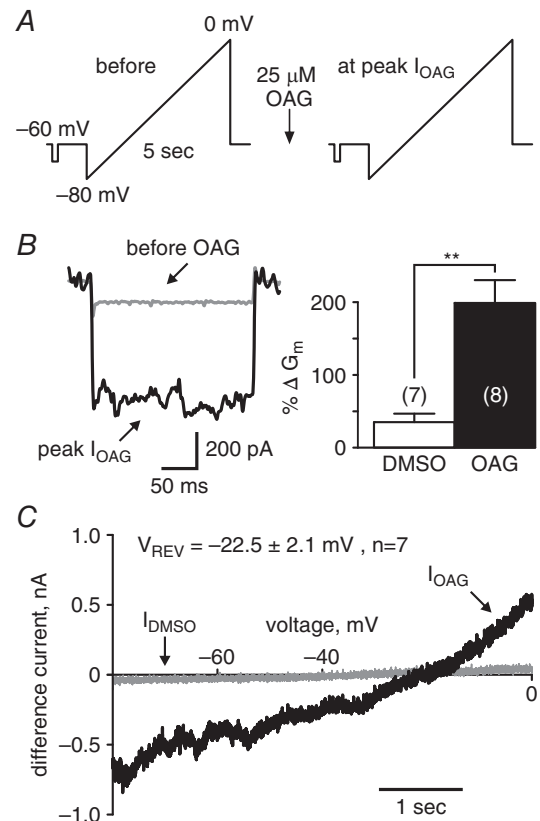


Figure 2. I_{OAG} is consistent with opening of a non-selective cation channel

A, voltage ramp protocol shows neurons are whole-cell voltage clamped at -60 mV in nASW with a Cs^+ -based intracellular solution to diminish any voltage-gated K^+ current. A 200 ms step to -70 mV is given, to determine membrane conductance (G_m), followed by a 5 s ramp from -80 to 0 mV to test reversal potential (V_{REV}). Subsequently, $25 \mu\text{M}$ OAG is added and, at peak I_{OAG} , the ramp protocol repeated. Difference current is calculated by subtracting the current before addition of OAG from the current at peak I_{OAG} . B, left, current produced by the pulse to -70 mV after OAG (black) is increased compared to before OAG (grey). Right, summary graph of the percentage change in conductance calculated from the step before and after DMSO or OAG. There is a significant increase following OAG ($198.8 \pm 31.4\%$) compared to DMSO ($35.1 \pm 11.7\%$) (** $P = 0.0012$, unpaired t test with Welch correction). C, examples of current-voltage relationships derived from ramp protocol subtractions in DMSO (grey) or OAG (black). The difference current ramp for DMSO is almost flat, while the ramp taken at peak I_{OAG} presents a V_{REV} of $-22.5 \pm 2.1 \text{ mV}$ ($n = 7$). V_{REV} calculated by fitting a straight line to a section of the current trace as it crosses 0 nA (see Methods for details).

black trace). For DMSO, no current was observed after delivery. Therefore, the 2nd ramp protocol was performed 5 min post DMSO, which was approximately the time of peak I_{OAG} . The difference current for DMSO was clearly smaller than OAG, with a V_{REV} of ~ -40 mV (Fig. 2C, grey trace).

I_{OAG} is blocked by cation channel blockers

We next used a pharmacological approach with general cation channel antagonists to provide further evidence that OAG activates a non-selective channel. We first employed Gd^{3+} , an established cation channel blocker (Yang & Sachs, 1989; Franco & Lansman, 1990; Popp *et al.* 1993; Chakfe & Bourque, 2000). A 20 min pretreatment with $1 \mu\text{M}$ Gd^{3+} ($n = 4$) did not reduce the current evoked by OAG in cultured bag cell neurons voltage-clamped at -60 mV (Fig. 3A, upper). However, incubation with $30 \mu\text{M}$ Gd^{3+} ($n = 4$) inhibited I_{OAG} , as did concentrations of $100 \mu\text{M}$ ($n = 4$), $300 \mu\text{M}$ ($n = 3$) and 1 mM ($n = 4$) (Fig. 3A, middle and lower, and C). The appearance of small flickers of current (~ -50 to -200 pA), as well as sharp current spikes (greater than -1.5 nA), was reduced with increasing concentrations of Gd^{3+} . Specifically, while I_{OAG} was activated following pretreatment with $1 \mu\text{M}$ Gd^{3+} , only small flickers and a sharp peak were visible with $30 \mu\text{M}$ pretreatment, and only one small flicker was seen at $300 \mu\text{M}$ (Fig. 3A).

We also tried the fenamate, flufenamic acid (FFA), which has been used as a general non-selective cation channel blocker (Gogelein & Pfannmuller, 1989; Gogelein *et al.* 1990; Shaw *et al.* 1995; Green & Cottrell, 1997; Haj-Dahmane & Andrade, 1997; Partridge & Valenzuela, 2000). Neurons given $100 \mu\text{M}$ FFA for 20 min exhibited a markedly reduced I_{OAG} caused by $25 \mu\text{M}$ OAG ($n = 9$) (Fig. 3B, upper), and the area above I_{OAG} was down 50%. Previous work from our lab suggests that one of the non-selective cation channels active during the after-discharge is similar to the TRPM subfamily (Lupinsky & Magoski, 2006; Gardam & Magoski, 2009). Hence, we introduced a so-called TRPM4-specific inhibitor, 9-phenanthrol (9-Pt) (Grand *et al.* 2008; Guinamard *et al.* 2014), and bath applied $25 \mu\text{M}$ OAG. However, delivery of OAG to neurons pretreated with 9-Pt for 20 min still resulted in a strong I_{OAG} ($n = 4$) (Fig. 3B, lower). The difference between the two blockers was significant (Fig. 3C).

I_{OAG} increases intracellular Ca^{2+}

Several non-selective cation channels, including those from bag cell neurons, are Ca^{2+} permeable (Lupinsky & Magoski, 2006; Gardam & Magoski, 2009; Geiger *et al.* 2009; Hickey *et al.* 2013). Thus, we sought to determine if I_{OAG} could change the level of $[\text{Ca}^{2+}]_i$ by using the Ca^{2+} -sensitive dye, fura-PE3 (Grynkiewicz *et al.* 1985;

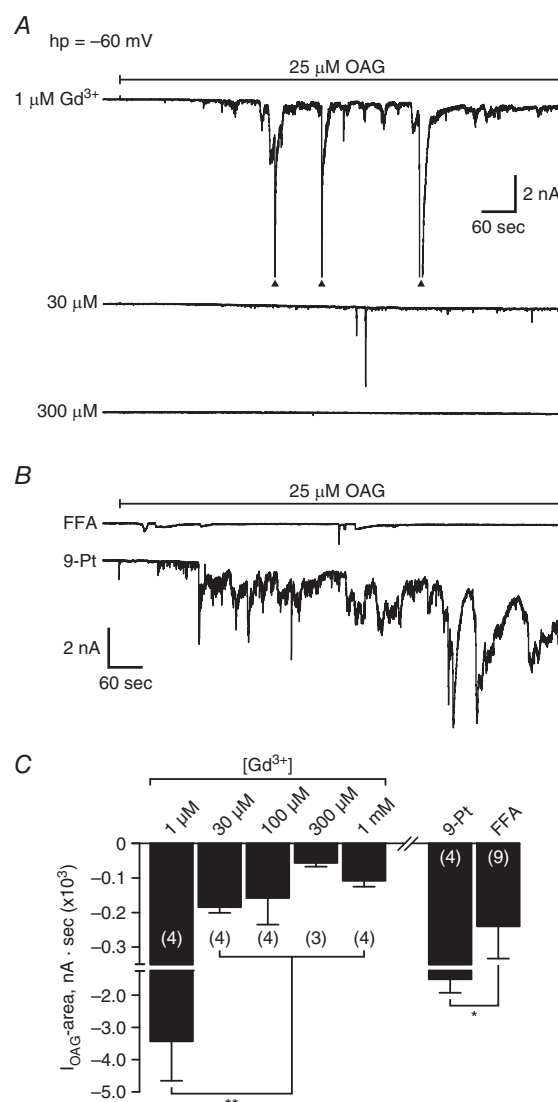


Figure 3. I_{OAG} is inhibited by Gd^{3+} or flufenamic acid (FFA), but not 9-phenanthrol (9-Pt)

A, current responses to $25 \mu\text{M}$ OAG (at bar) of different cultured bag cell neurons whole-cell voltage-clamped at -60 mV after 20 min pretreatment with increasing concentrations of Gd^{3+} (as indicated). At $1 \mu\text{M}$, Gd^{3+} does not alter I_{OAG} , whereas Gd^{3+} concentrations higher than $1 \mu\text{M}$ noticeably reduce the current. Scale bars apply to all traces. Arrowheads indicate truncation of currents for display. B, representative responses to OAG in neurons incubated with $100 \mu\text{M}$ FFA (upper) or $100 \mu\text{M}$ 9-Pt (lower) for 20 min. FFA largely ablates I_{OAG} , while 9-Pt has no obvious impact. C, summary concentration-response graph of I_{OAG} -area in Gd^{3+} , FFA, or 9-Pt. Pretreating with $1 \mu\text{M}$ Gd^{3+} still yields a strong I_{OAG} (-3427.8 ± 1225.4 nA·s), while higher Gd^{3+} concentrations ($30 \mu\text{M}$, $100 \mu\text{M}$, $300 \mu\text{M}$ and 1 mM) result in almost no change in holding current to OAG ($30 \mu\text{M} = -184.7 \pm 16.3$; $100 \mu\text{M} = -158.2 \pm 76.5$; $300 \mu\text{M} = -56.3 \pm 10.8$; $1 \text{ mM} = -108.41 \pm 17.1$ (all quantified as nA·s)) ($P = 0.0033$, standard ANOVA; $**P < 0.01$, Student–Newman–Keuls test compared to $1 \mu\text{M}$ control). Area above I_{OAG} in cells exposed to 9-Pt (-1506.6 ± 417.2 nA·s) are notably large, but the presence of FFA results in inhibition of I_{OAG} (-239.8 ± 93.4 nA·s) ($*P = 0.0112$, Mann–Whitney unpaired U test).

Vorndran *et al.* 1995). With 1 mM fura-PE3 in the intracellular saline, we dialysed cultured bag cell neurons for 20 min then simultaneously measured $[Ca^{2+}]_i$ and membrane current in response to OAG under voltage clamp at -60 mV (see Fig. 4D, lower panel, for example of region of interest used to measure fura fluorescence). The neurons exhibited no current following DMSO, and the fura fluorescence ratio (340/380) did not increase (Fig. 4A). Neurons exposed to $25 \mu\text{M}$ OAG, however, exhibited I_{OAG} and concomitant increases in $[Ca^{2+}]_i$ (Fig. 4B). Specifically, comparing the fura ratio during I_{OAG} revealed that following a sharp peak in membrane current there was a correlated increase in $[Ca^{2+}]_i$. With the application of OAG, the peak change in the fura ratio represented an $\sim 100\%$ increase compared to baseline, whereas in DMSO the peak change was an $\sim 10\%$ decrease in the ratio (Fig. 4C). Regarding the average Ca^{2+} level, OAG lead to a mean fura ratio of 0.498 ± 0.06 ($n = 10$) while DMSO gave 0.238 ± 0.003 ($n = 7$) when calculated over the entire time that the neurons were in the presence of drug or vehicle.

Phospholipase C activation mimics I_{OAG} , which is augmented by IP_3

Having demonstrated that I_{OAG} probably constitutes a non-selective current, we next sought to determine if directly turning on PLC was sufficient to release adequate amounts of DAG to trigger a similar current. Bath application of a PLC activator, *m*-3M3FBS (Bae *et al.* 2003), to whole-cell voltage-clamped cultured bag cell neurons evoked an inward current in a dose-dependent manner. This PLC activator, previously shown to effectively increase neurite outgrowth in *Aplysia* bag cell neurons (Zhang *et al.* 2012), caused an inward current similar, though ostensibly smaller in magnitude, to I_{OAG} . This was apparent at concentrations of $10 \mu\text{M}$ ($n = 5$) and $25 \mu\text{M}$ ($n = 10$) *m*-3M3FBS (Fig. 5B, middle and lower); in contrast, $3 \mu\text{M}$ *m*-3M3FBS (Fig. 5B, upper) or $25 \mu\text{M}$ of the inactive isoform, *o*-3M3FBS ($n = 9$), failed to elicit a current (Fig. 5A). Similar to I_{OAG} , the area above the *m*-3M3FBS current increased with larger concentrations and was significantly higher compared to *o*-3M3FBS (Fig. 5C). The latency of the current elicited by *m*-3M3FBS (308.1 ± 77.6 s; $n = 5$) was much slower than that of I_{OAG} (see above). To examine if the effects of OAG and *m*-3M3FBS were additive, where *m*-3M3FBS would liberate the endogenous DAG and OAG would exogenously activate the current, we bath applied $25 \mu\text{M}$ *m*-3M3FBS and $25 \mu\text{M}$ OAG in close succession. However, this resulted in the cells becoming overwhelmed with inward current, eventually leading to cell death ($n = 5$) (data not shown).

The activity of PLC increases during the afterdischarge, boosting the levels of both DAG and IP_3 . While the effects

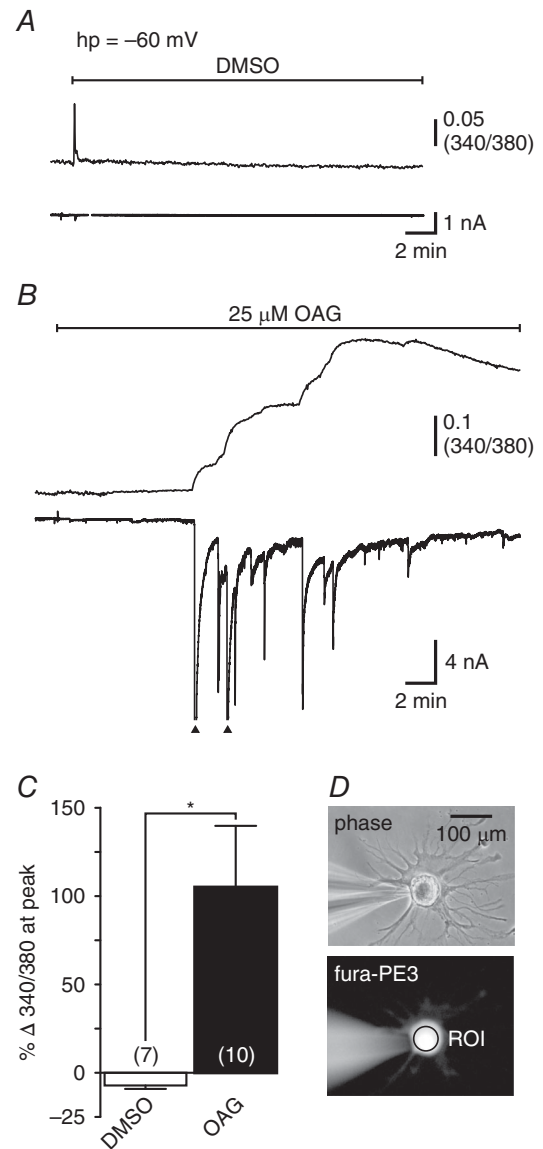


Figure 4. I_{OAG} induces a rise in $[Ca^{2+}]_i$

A, simultaneous measurement of free $[Ca^{2+}]_i$ (upper) and membrane current (lower) in cultured bag cell neurons using 340/380 fura PE3 fluorescence and whole-cell voltage-clamp at -60 mV. Addition of DMSO (at bar) causes no clear change in $[Ca^{2+}]_i$ or membrane current. Time base applies to both traces. However, delivering $25 \mu\text{M}$ OAG (B) elevates Ca^{2+} (upper), with concomitant increases in I_{OAG} (lower). Note that the sharp peaks in I_{OAG} often correspond with inflection points on the Ca^{2+} trace. Arrowheads indicate current truncation for display. Time base applies to both traces. C, summary graph of the percentage change of the 340/380 fura PE3 fluorescence, from initial level to peak, in cells treated with DMSO ($-7.2 \pm 1.9\%$) or OAG ($105.0 \pm 34.7\%$) shows OAG significantly increases the free Ca^{2+} concentration ($*P = 0.0103$, unpaired *t* test with Welch correction). D, upper panel, a phase contrast image shows the recording pipette (left side of the photomicrograph), bag cell neuron soma and its neurites. Lower panel, the same neuron loaded with fura and excited at 340 nm, with the region of interest (ROI) used for data collection. Focal plane of both images approximately half-way up the vertical axis of the soma. Scale bar applies to both images.

of IP₃ as a Ca²⁺ release agent in cultured bag cell neurons have been documented (Fink *et al.* 1988), we wanted to test if IP₃ combined with DAG could interact and affect whole-cell current. For these experiments, the solution in the recording electrode contained 5 μM IP₃. Following bath application of 25 μM OAG, under voltage clamp at -60 mV, inclusion of IP₃ significantly increased I_{OAG} (Fig. 5D). With IP₃, I_{OAG} showed a significantly larger area above the current compared to standard internal saline in the electrode (Fig. 5E). With IP₃ in the internal solution, the holding current did not recover to the same extent as in the absence of IP₃ (-0.5 to -1 nA), often only returning to ~-2 nA following I_{OAG} (data not shown).

I_{OAG} requires basal PKC activity

DAG is capable of activating PKC in certain tissues (Berridge & Irvine, 1984; Nishizuka, 1984). Thus, we sought to address the distinct possibility that OAG is activating PKC in bag cell neurons, and this is responsible for I_{OAG}. Therefore, we incubated cultured neurons for 20 min with the PKC inhibitors Bis, sphinganine, or H7 (Hidaka *et al.* 1984; Hannun *et al.* 1986; Toullec *et al.* 1991), all of which are effective in *Aplysia* (Conn *et al.* 1989a,b; Zhang *et al.* 2002; Villareal *et al.* 2009; Tam *et al.* 2011), and bath applied 25 μM OAG (Fig. 6A). Following each inhibitor, I_{OAG} was significantly reduced (Fig. 6A,

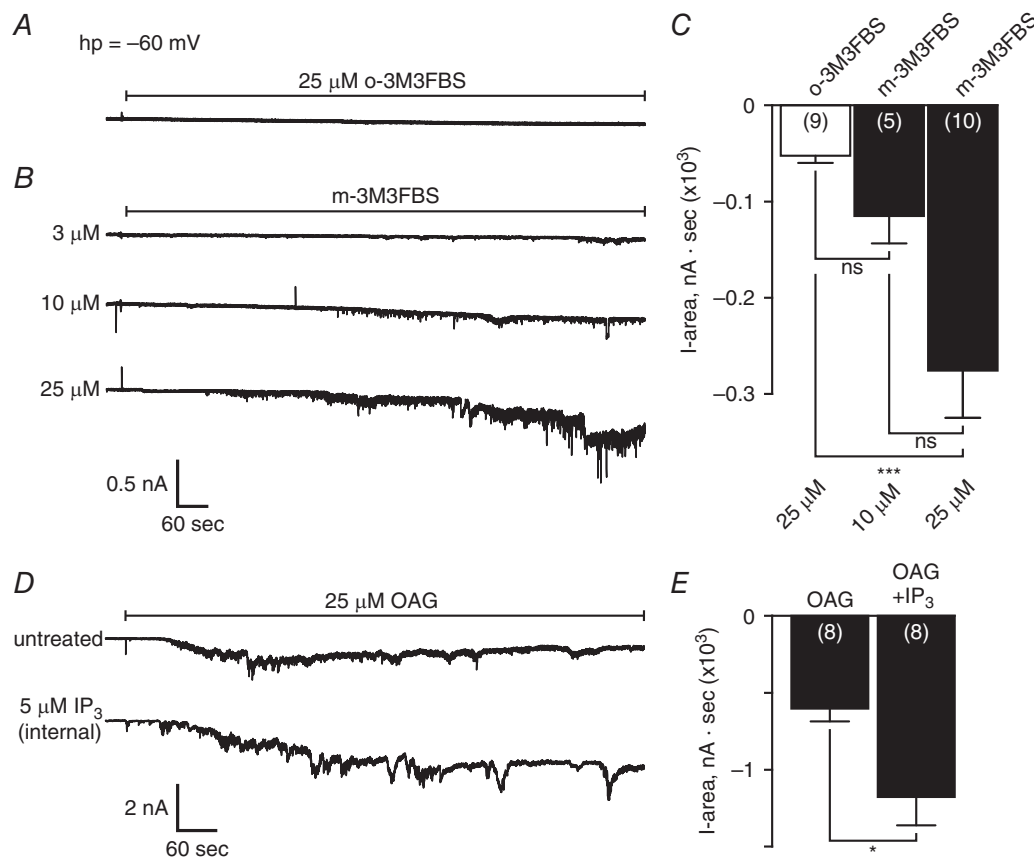


Figure 5. PLC activation evokes an inward current, which is enhanced by IP₃ in cultured bag cell neurons

A, whole-cell voltage-clamp recording at -60 mV shows bath-applying 25 μM of an inactive analogue, o-3M3FBS (at bar), has no effect on current. **B**, addition of the PLC activator, m-3M3FBS, at the indicated concentrations, induces an inward current starting at 10 μM. The current, though weaker in magnitude and longer in latency, is qualitatively similar to I_{OAG}. Scale bars apply to both **A** and **B**. **C**, summary graph of area above the o-3M3FBS- (-52.3 ± 7.6 nA · s) or m-3M3FBS-induced current (10 μM = -115.2 ± 28.5; 25 μM = -275.9 ± 49.1 (all quantified as nA · s)) reveals a concentration-dependent effect like that of I_{OAG} ($P = 0.0003$, KW ANOVA; *** $P < 0.001$, Dunn's multiple comparisons test). **D**, bath application of 25 μM OAG to untreated neurons dialysed with normal intracellular solution (upper) evokes a typical I_{OAG}, while using intracellular solution containing 5 μM IP₃ (lower) produces a significantly enhanced response. **E**, summary graph of the area above the current shows that I_{OAG} is significantly larger with inclusion of IP₃ in internal saline (-1177.0 ± 184.4 nA · s) compared to 25 μM OAG (data reproduced from Fig. 1C) (* $P = 0.0131$, unpaired *t* test).

upper, upper-middle and middle), with the area above I_{OAG} in 100 nM Bis ($n = 7$), 20 μM sphinganine ($n = 6$) or 100 μM H7 ($n = 6$) being less than 20% of DMSO-treated neurons ($n = 5$) (Fig. 6A, lower, and B). In addition, and consistent with PKC being necessary, but not sufficient to activate I_{OAG} , when we pretreated neurons with 100 nM of the PKC activator, phorbol 12-myristate 13-acetate (PMA) (Castagna *et al.* 1982), which is a potent stimulator of PKC in *Aplysia* (DeRiemer *et al.* 1985c; Sossin *et al.* 1993; Tam *et al.* 2011), the response to 25 μM OAG was not significantly different from DMSO-exposed neurons (Fig. 6A, lower-middle and lower, and B).

Reduction of I_{OAG} by PKC inhibitors provides evidence of the involvement of PKC. However, addition of H7

at onset or peak of I_{OAG} did not inhibit the current. Specifically, we delivered 25 μM OAG to untreated bag cell neurons, and added 100 μM H7 several minutes after the onset of I_{OAG} , yet there was no effect on the current, nor an immediate return to baseline membrane holding current (Fig. 6C, upper). The area above I_{OAG} in these experiments was not significantly different from control experiments in which H_2O was added after current onset (Fig. 6C, lower, and D).

PKC activation does not trigger I_{OAG}

Because I_{OAG} is reduced by PKC inhibition prior to OAG exposure, we investigated if activation of PKC,

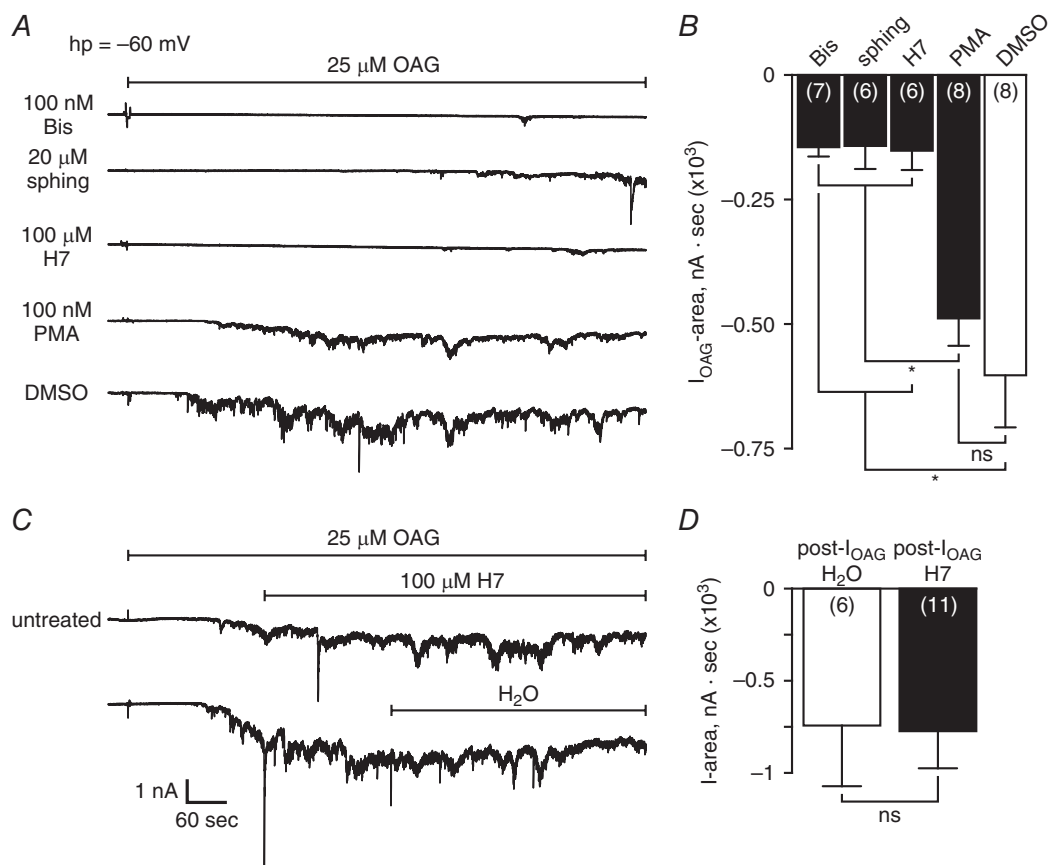


Figure 6. I_{OAG} is prevented by pretreatment with PKC inhibitors Bis, sphinganine and H7, but delivering H7 post current onset does not block I_{OAG}

A, whole-cell voltage-clamp recording at -60 mV of bath application of 25 μM OAG (at bar) to neurons pretreated for 20 min with either 100 nM bisindolylmaleimide I (Bis, upper), 20 μM sphinganine (sphing, upper-middle) or 100 μM H7 (middle) evokes very little current compared to DMSO (lower). Pretreatment of the bag cell neurons with 100 nM PMA (lower-middle) does not significantly alter I_{OAG} . B, summary I_{OAG} -area graph in neurons pretreated with PKC blockers or PMA (DMSO = -602.6 ± 104.6 ; PMA = -488.7 ± 54.7 ; H7 = -152.0 ± 38.6 ; sphing = -142.4 ± 46.1 ; Bis = -144.6 ± 18.8 (all quantified as nA · s)) ($P = 0.0002$, KW ANOVA; * $P < 0.05$, Dunn's multiple comparisons test). C, voltage-clamp recordings of two different neurons showing current elicited by 25 μM OAG, followed by either 100 μM H7 or water (the vehicle) shortly after the onset of I_{OAG} . The addition of H7 causes no obvious reduction in current (upper); similarly, introducing H_2O also has little impact on the response (lower). D, group data reveal that delivery of H7 post- I_{OAG} results in a typical area above the current (-772.8 ± 201.7 nA · s). H_2O as a control results in a similar effect (-741.8 ± 330.0 nA · s) ($P = 0.9333$; unpaired t test). Scale bars apply to A and C.

independent of OAG, would yield a current similar to I_{OAG} . Under whole-cell voltage clamp at -60 mV, cultured bag cell neurons were exposed to 100 nM PMA; however, PMA did not lead to significant change in current or area above holding current (-100.8 ± 31.1 nA \cdot s; $n = 7$) (Fig. 7A).

Thus far, our results suggest OAG does not trigger PKC; rather, the induction of I_{OAG} requires PKC activity prior to onset. To provide further evidence that OAG does not turn on PKC in our hands, we employed a Ca^{2+} current bioassay and compared it to PMA. PMA is well established as being capable of enhancing the voltage-dependent Ca^{2+} currents of cultured bag cell neurons in a PKC-dependent manner (DeRiemer *et al.* 1985c; Strong *et al.* 1987b; Conn *et al.* 1989b; Zhang *et al.* 2008; Tam *et al.* 2009; Groten & Magoski, 2015). Voltage-gated currents were elicited by 200 ms voltage steps in 10 mV increments from -60 to $+40$ mV in neurons bathed in Ca^{2+} - Cs^+ -TEA-ASW and dialysed with Cs^+ -Asp-based intracellular saline. Neurons presented Ca^{2+} currents with an onset voltage of -20 mV and maximum amplitude at $+10$ mV (Fig. 7C). Currents recorded after a 20 min DMSO pretreatment ($n = 14$) (Fig. 7B, upper) were no different from those in neurons exposed to 25 μ M OAG ($n = 17$) (Fig. 7B, middle). However, incubating with 100 nM PMA lead to a clear enhancement of Ca^{2+} current ($n = 13$) (Fig. 7B, lower). The impact of PMA on the current was significant compared to both OAG and DMSO, particularly in the range of -20 to $+30$ mV, where we found the strongest Ca^{2+} current (Fig. 7C).

PLC activation and OAG depolarize cultured bag cell neurons

Given that PLC is triggered during the afterdischarge (Fink *et al.* 1988), and either PLC activation or OAG application evokes inward current, we sought to determine the impact of introducing m -3M3FBS or OAG on the membrane potential of cultured bag cell neurons from a resting potential of -60 mV under sharp-electrode current clamp in nASW. As expected, the vehicle, DMSO ($n = 5$) (Fig. 8A), and the inactive form of the PLC activator, o -3M3FBS ($n = 8$) (Fig. 8B, upper), both failed to depolarize the neurons. Activation of PLC using 25 μ M m -3M3FBS caused an ~ 30 mV depolarization ($n = 10$) (Fig. 8B, lower). In some neurons ($n = 2$ of 10), m -3M3FBS evoked a short period of action potential firing with a frequency of ~ 0.3 Hz and a mean spike amplitude of 50 mV ($n = 5$). In these neurons that exhibited action potentials, the voltage during the depolarization was determined by fitting an all-points histogram of membrane potential (see Methods for details).

Delivery of 25 μ M OAG to cultured bag cell neurons caused a similar depolarization of close to 30 mV ($n = 8$) (Fig. 8D, upper, and E); however, prolonged action potential firing, with a mean frequency of 1.2 ± 0.3 Hz

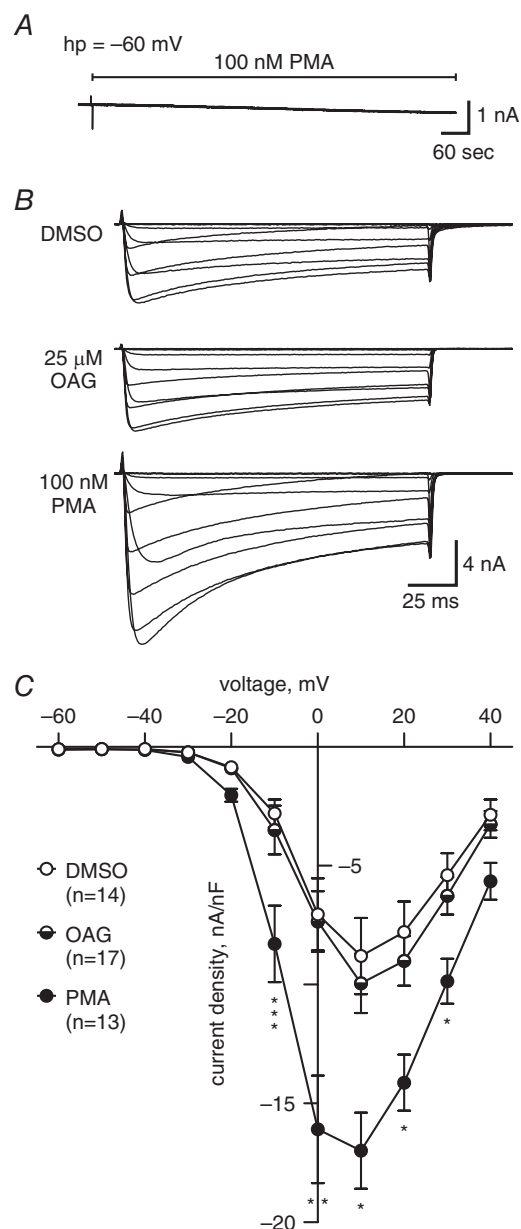


Figure 7. The PKC activator, PMA, increases Ca^{2+} currents in cultured bag cell neurons, but OAG does not

A, whole-cell voltage-clamp recording of bath application (at bar) of 100 nM PMA to a cultured bag cell neuron held at -60 mV shows no change in current. B, traces of voltage-gated Ca^{2+} currents evoked with 200 ms, 10 mV incremental square pulses from -60 mV to $+40$ mV in Ca^{2+} - Cs^+ -TEA-ASW external with Cs^+ -Asp-based internal from neurons pretreated with DMSO (upper), 25 μ M OAG (middle), or 100 nM PMA (lower) for 20 min. The currents in PMA are noticeably bigger at most test potentials. Scale bars apply to all traces. C, summary graph of the current-voltage relationship for Ca^{2+} current in the three conditions. Peak current at each voltage is normalized to whole-cell capacitance and reported as current density. Comparing the current densities at each voltage shows PMA (filled circles), but not OAG (half-filled circles) or DMSO (open circles), enhances Ca^{2+} current elicited by steps to -20 through to $+30$ mV ($P = 0.0062$, KW ANOVA; $*P < 0.05$, $**P < 0.01$, $***P < 0.001$, Dunn's multiple comparisons test).

($n = 6$) and spike amplitude between 70 and 80 mV, was observed in most of the neurons tested ($n = 6$ of 8). To test if PKC was involved with the OAG-induced membrane depolarization, OAG was delivered to neurons pretreated for 20 min with 100 μM H7 (Fig. 8D, lower). In these cells, there was an ~ 12 mV depolarization ($n = 6$), which was significantly smaller than that induced by OAG alone (Fig. 8E). Out of the eight neurons given H7 and subsequently exposed to OAG, only two began to fire action potentials, and in both of those cells the firing lasted less than 2 min, unlike OAG, which exhibited periods of spiking of 10–30 min.

OAG prolongs evoked afterdischarges in intact bag cell neuron clusters

Having established that bag cell neurons respond to OAG with a prolonged inward current or membrane

depolarization coupled with action potential firing, we explored the effects of OAG on the intact bag cell neuron cluster. In these experiments, we used an extracellular recording electrode to monitor the activity of the entire cluster, while a second extracellular electrode served to stimulate the ipsilateral connective nerve, and sharp-electrode current-clamp intracellular recording from a single neuron in the desheathed, contralateral cluster (Fig. 9A, inset; see Methods for details). In 10 different clusters, bath application of 25 μM OAG failed to evoke an afterdischarge on its own, nor did it cause an obvious depolarization of any individual neurons recorded from the cluster. Unsurprisingly, addition of DMSO also failed to evoke an afterdischarge ($n = 7$).

However, when afterdischarges were triggered via electrical stimulation of the connective nerve following OAG application, the mean duration was more than 50 min ($n = 4$), compared to ~ 25 min for afterdischarges

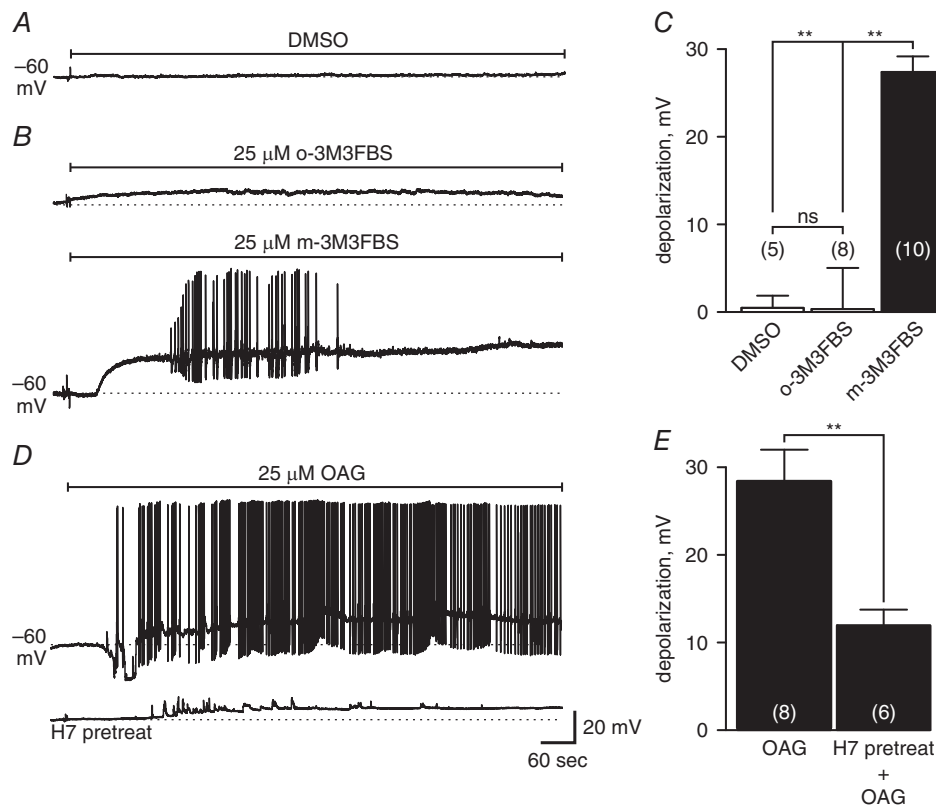


Figure 8. PLC activation and OAG depolarize cultured bag cell neurons

A, in nASW under sharp-electrode current-clamp, with the neurons set to -60 mV (dashed line) with bias current, bath application of DMSO (at bar) does not affect membrane voltage. B, at 25 μM the PLC activator *m*-3M3FBS depolarizes a bag cell neuron (lower), while the inactive isoform *o*-3M3FBS has no appreciable effect (upper). Addition of *m*-3M3FBS induces action potential firing in 2 out of 10 neurons tested. C, summary graph indicating the average depolarization induced by *m*-3M3FBS (27.4 ± 1.8 mV) differs significantly from both DMSO (0.5 ± 1.4 mV) and the inactive *o*-3M3FBS (0.3 ± 4.7 mV) ($P < 0.0001$, KW ANOVA; $**P < 0.01$, Dunn's multiple comparisons test). D, upper trace, bath application of 25 μM OAG induces membrane depolarization. Lower trace, exposing the neurons to the PKC inhibitor H7 (100 μM) results in a markedly reduced depolarization upon addition of OAG. Scale bars apply to A, B and D. E, summary graph indicates that the difference between the OAG-induced depolarization amplitude for untreated neurons (28.4 ± 3.6 mV) and neurons incubated in H7 for 20 min (11.9 ± 1.8 mV) is significant ($**P = 0.0027$, Mann-Whitney *U* test).

stimulated subsequent to the addition of DMSO ($n = 4$) (Fig. 9A). The length of afterdischarges following OAG was significantly longer than following DMSO (Fig. 9B). In addition, two of the four clusters stimulated to afterdischarge in OAG could, once they had stopped spiking, be further stimulated to fire a second afterdischarge of 7 and 22 min, respectively. This was not the case following afterdischarges in DMSO. The action potentials in the OAG-exposed clusters (measured with intracellular recording) were also sooner to peak (~ 31 ms) in the fast phase of the afterdischarge, compared to DMSO (~ 53 ms), and the action potential amplitude was slightly larger (~ 86 mV in OAG vs. ~ 75 mV in DMSO) (Fig. 9C).

Discussion

In the present study, we examined the effects of OAG, a synthetic, membrane-permeable DAG analogue,

on cultured bag cell neurons. Bath applied OAG evokes a slow, dose-dependent, inward current in whole-cell voltage-clamp recordings. I_{OAG} is consistently activated by the drug, but varies in terms of latency and amplitude. Another membrane-permeable DAG analogue, DOG, mimics the effect of OAG, while a membrane-impermeable analogue, SAG, has no effect. The inability of the membrane-impermeable SAG to elicit current is equivalent to that observed by Hofmann *et al.* (1999) for TRPC6-expressing cell lines, and is consistent with OAG acting intracellularly. OAG has been shown to elicit a comparable, noisy current in rabbit portal vein smooth muscle cells (Helliwell & Large, 1997; Albert & Large, 2003), and while the *Aplysia* and rabbit currents appear qualitatively similar, we demonstrate a requirement for basal PKC activity to trigger I_{OAG} . To our knowledge, this finding represents the only report of an OAG-induced current requiring, but not being directly activated by, PKC activity.

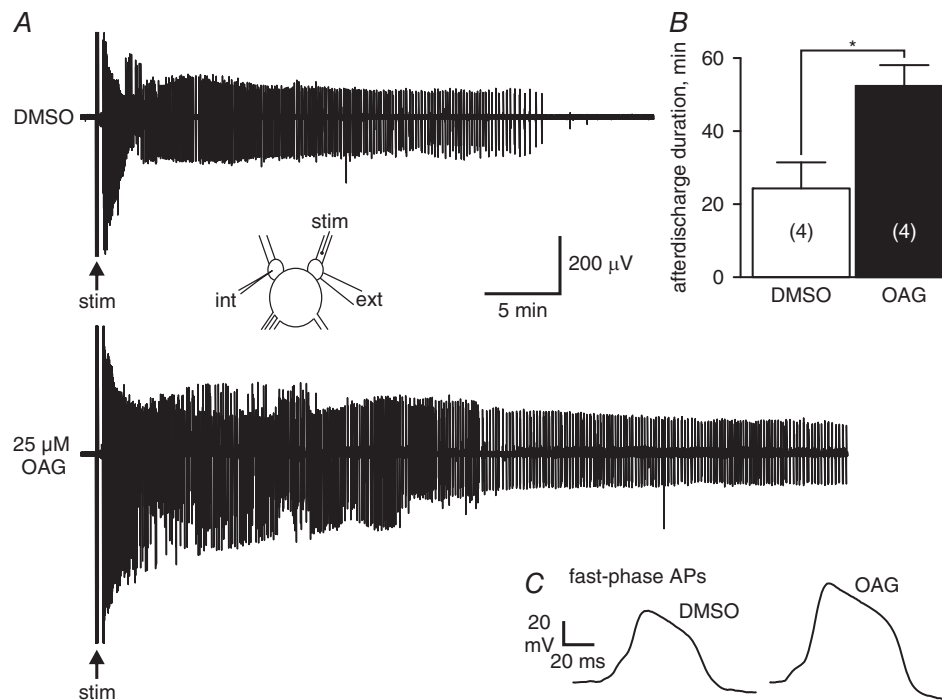


Figure 9. OAG prolongs electrically stimulated afterdischarges of intact bag cell neuron clusters in the abdominal ganglion

A, ensemble extracellular recordings (inset) from separate bag cell neuron clusters bathed in nASW following stimulation of the ipsilateral pleuroabdominal connective (stim) in the presence of DMSO or $25 \mu\text{M}$ OAG. Upper trace, in DMSO, a train stimulus (10 ms, 20 V at 5 Hz for 10 s; at arrow) to the afferent input elicits an afterdischarge, with a typical fast and slow phase that represents the synchronous firing of all of the cells in the cluster. Lower trace, in a cluster to which OAG has been applied, the same stimulation elicits an afterdischarge that is far longer. The extracellular action potential amplitude is also higher in those neurons exposed to OAG. Recordings truncated at 38 min (upper) and 51 min (lower) for display. Scale bars apply to both traces. B, mean duration of synaptically stimulated afterdischarges following OAG (52.4 ± 5.7 min) is longer than in DMSO-treated clusters (24.3 ± 7.1 min) ($*P = 0.0277$, unpaired t test with Welch correction). C, intracellular recordings (see A, inset) of action potentials (APs) from individual bag cell neurons in two different clusters during the fast phase of the afterdischarge. The spike of a neuron in a DMSO-exposed cluster (left) has a smaller amplitude than that in a cluster exposed to OAG (right). Scale bars apply to both traces.

As with previous reports from our laboratory regarding cation currents gated by acetylcholine, intracellular Ca^{2+} , or phosphorylation (Hung & Magoski, 2007; Gardam *et al.* 2008; Hickey *et al.* 2010; White & Magoski, 2012), OAG increases membrane conductance and reverses close to -20 mV, suggesting it too carries cations non-selectively. In addition, activation of I_{OAG} also causes a marked elevation in $[\text{Ca}^{2+}]_i$, punctuated by sharp increases in the fura ratio synchronized with large spikes of I_{OAG} . The latter in particular is probably the result of Ca^{2+} influx through an OAG-gated cation channel, rather than Ca^{2+} release from an intracellular store. Also, the -60 mV holding potential used during fura imaging would prevent activation of any voltage-dependent Ca^{2+} current (Tam *et al.* 2009).

I_{OAG} is blocked by $100 \mu\text{M}$ FFA, a general cation channel blocker (Shaw *et al.* 1995; Green & Cottrell, 1997; Haj-Dahmane & Andrade, 1997; Partridge & Valenzuela, 2000). We also found that $\geq 30 \mu\text{M}$ Gd^{3+} , another common cation channel blocker (Yang & Sachs, 1989; Franco & Lansman, 1990; Popp *et al.* 1993), inhibited I_{OAG} . In bag cell neurons, a key conductance that maintains the afterdischarge is a Ca^{2+} - and voltage-dependent cation channel, which is modulated by calmodulin and PKC (Wilson *et al.* 1998; Magoski & Kaczmarek, 2005; Lupinsky & Magoski, 2006; Gardam & Magoski, 2009). These characteristics have also been attributed to TRPM4 and M5 channels (Launay *et al.* 2002; Hofmann *et al.* 2003; Liu & Liman, 2003); however, the lack of voltage-gating or direct effect of PKC on I_{OAG} suggests I_{OAG} and the other bag cell neuron cation currents are carried by discrete channels. Accordingly, I_{OAG} is not blocked by the TRPM4-specific inhibitor 9-Pt (Grand *et al.* 2008; Guinamard *et al.* 2014). More likely, OAG (and endogenously, DAG) may open a member of the TRPC family, as described in expression systems and cerebellar Purkinje neurons (Hofmann *et al.* 1999; Kim SJ *et al.* 2003; Dietrich *et al.* 2005; Kim Y *et al.* 2012).

The level of membrane noise seen during I_{OAG} made us consider whether the cells were still healthy following drug. Naive cultured bag cell neurons exhibit a large inward current in response to acetylcholine by the opening of an ionotropic cholinergic receptor (White & Magoski, 2012; White *et al.* 2014); moreover, we find that post- I_{OAG} neurons respond similarly upon acetylcholine delivery. The current, however, was significantly stronger than that reported by White & Magoski (2012) (-40 vs. -4 pA pF $^{-1}$). We also used a second acetylcholine pressure ejection to examine receptor desensitization. We previously found a 50–60% desensitization (White & Magoski, 2012; White *et al.* 2014), yet in the present study, the second acetylcholine current was almost 80% of the first current, suggesting OAG may potentiate the acetylcholine receptor. The presence of other membrane lipids, such as phosphatidic acid or cholesterol, can

influence nicotinic receptors (Sturgeon & Baenziger, 2010), stabilizing a resting state over the desensitized conformation (daCosta *et al.* 2002).

The OAG current seen in other reports is PKC independent (Helliwell & Large, 1997; Hofmann *et al.* 1999), but we found that blocking PKC with either Bis, H7, or sphinganine, prevented I_{OAG} in bag cell neurons. All of these inhibitors are structurally distinct and have been used extensively to occlude PKC in *Aplysia* for many years (DeRiemer *et al.* 1985b; Conn *et al.* 1989a,b; Loechner *et al.* 1992; Zhang *et al.* 2002; Villareal *et al.* 2009; Tam *et al.* 2011). Phosphorylation and whole-cell analyses of bag cell neuron kinases point to H7 being selective for PKC over protein kinase A (PKA) (Conn *et al.* 1989a), although *in vitro* assays of rabbit enzymes indicate that H7 can block both PKC and PKA (Hidaka *et al.* 1984). Sphinganine was first found to inhibit PKC from platelets (Hannun *et al.* 1986) but subsequently seen to also inhibit sphingosine kinase (Buehrer & Bell, 1992). Hence, the action of these reagents should be interpreted with some caution. That aside, Bis appears to be highly selective for PKC (Toullec *et al.* 1991), including that of *Aplysia* (Villareal *et al.* 2009), suggesting that PKC inhibition is indeed responsible for preventing I_{OAG} .

OAG could very well turn on PKC (Nishizuka, 1984; Kaczmarek, 1986), so the notion that I_{OAG} in these cells is related to PKC activity is logical. However, the PKC activator PMA (Castagna *et al.* 1982; Sossin *et al.* 1993) does not provoke an inward current as per OAG; yet, unlike OAG, PMA clearly enhances rapid, voltage-gated Ca^{2+} currents in a manner similar to numerous previous reports (DeRiemer *et al.* 1985c; Tam *et al.* 2011; Groten & Magoski, 2015). The PMA-induced elevation of Ca^{2+} current is also prevented by pretreating with PKC inhibitors (Conn *et al.* 1989a,b; Tam *et al.* 2011; Groten & Magoski, 2015), and the effect of PMA on the Ca^{2+} component of the action potential is mimicked by intracellular injection of PKC enzyme (DeRiemer *et al.* 1985a). Parenthetically, Strong *et al.* (1987a) show that DOG, a known PKC activator, enhances Ca^{2+} -dependent spikes, but does not cause depolarization or afterdischarge-like bursting.

The attenuation of I_{OAG} by PKC inhibitors, the failure of PMA to provoke I_{OAG} , and the inability of OAG to ostensibly activate PKC, all suggest that, while PKC alone cannot open the channel, the kinase is required for OAG-mediated gating. If PKC activity is a prior requirement for I_{OAG} , then any variability in current amplitude or latency could be due to differences in basal levels of PKC activity priming I_{OAG} to a different extent between neurons. The lack of inhibition with H7 delivered post-OAG suggests that PKC inhibition must occur prior to OAG addition, and that basal PKC is sufficient to prime I_{OAG} . However, we must acknowledge the separate possibility that OAG interacts with a PKC isoform different

from that interacting with PMA. There are two isoforms of PKC found within bag cell neurons: a Ca^{2+} -dependent Apl I and a Ca^{2+} -independent Apl II (Sossin *et al.* 1996; Nakhost *et al.* 1998). While PMA is able to activate both isoforms of PKC (Sossin *et al.* 1993), OAG may only activate a particular isoform, which may not be responsible for modulating Ca^{2+} current. Unfortunately, there are no known PKC inhibitors that differentiate the two isoforms.

Inclusion of IP_3 in the pipette solution results in amplification of I_{OAG} , and an increased number of sharp peaks of current, which has been shown for OAG-induced current in other tissues (Albert & Large, 2003; Ju *et al.* 2010). The synergy between IP_3 and OAG could play a role in maintenance of the fast phase of the afterdischarge. IP_3 mobilizes Ca^{2+} release from intracellular stores in *Aplysia* (Sawada *et al.* 1989; Chameau *et al.* 2001; Jin & Hawkins, 2003), while I_{OAG} causes Ca^{2+} influx, both of which could add to voltage-gated Ca^{2+} influx, and further ELH secretion.

Activation of PLC using *m*-3M3FBS in cultured bag cell neurons causes a current qualitatively similar, though smaller in magnitude, to I_{OAG} . The size of the *m*-3M3FBS-evoked current is probably linked to the concentration of PIP_2 in the membrane, which in turn impacts the amount of DAG released. In *Aplysia* neural tissue, inositol-containing phospholipids and phosphatidylserine constitute less than 25% of the total membrane lipids (Piomelli *et al.* 1987*a,b*). Thus, the membrane level of PIP_2 is presumably lower than $25 \mu\text{M}$, the concentration of OAG primarily used in the present study, and the lower amplitude of the *m*-3M3FBS-evoked current is probably a corollary of the amount of PIP_2 . There is also a slower time to activation for the *m*-3M3FBS current, which could reflect the additional time required for *m*-3M3FBS to cross the membrane and target PLC. Overall, the PLC pathway probably contributes to an increase in IP_3 , and elevated $[\text{Ca}^{2+}]_i$ throughout the afterdischarge, but could also bolster the initial Ca^{2+} influx.

The afterdischarge begins with acetylcholine-evoked membrane depolarization and a fast phase of action potential firing, resulting in a rapid rise of $[\text{Ca}^{2+}]_i$ (Fisher *et al.* 1994; Michel & Wayne, 2002; Tam *et al.* 2009; White & Magoski, 2012). We establish that PLC activation, using *m*-3M3FBS, or OAG exposure, depolarizes bag cell neurons and elicits prolonged action potential firing with a pattern similar to the afterdischarge of the entire bag cell cluster. To a lesser extent, *m*-3M3FBS increases excitability, although action potential firing occurs in fewer cells and to a reduced extent by comparison to the OAG. The fact that OAG or PLC activation both evoke inward current and depolarize bag cell neurons encouraged us to investigate OAG in bag cell neurons within the abdominal ganglia. Unlike acetylcholine, a known trigger of the afterdischarge (White & Magoski, 2012), OAG does not elicit bursting in the intact cluster. However, following exposure to OAG,

synaptically stimulated afterdischarges are significantly longer than controls. Moreover, the length of our control afterdischarges was essentially the same as reported previously, i.e. around 30 min (Kupfermann & Kandel, 1970; Conn & Kaczmarek, 1989; White & Magoski, 2012; Dargaei *et al.* 2014).

Potentially, the activity of PKC in cultured neurons may be sufficient to permit I_{OAG} to provoke firing, whereas in the intact cluster, basal PKC activity is not adequate to prime an OAG-induced afterdischarge. Nevertheless, when PKC is activated during a *bona fide* afterdischarge, the presence of exogenous OAG (and presumably I_{OAG}) provides additional depolarizing drive, thereby prolonging firing. *In vivo*, the current gated by DAG, possibly in concert with IP_3 , may combine with cholinergic and voltage-gated cation currents to maintain the afterdischarge, thus ensuring ELH secretion and reproductive behaviour.

References

- Albert AP & Large WA (2003). Synergism between inositol phosphates and diacylglycerol on native TRPC6-like channels in rabbit portal vein myocytes. *J Physiol* **552**, 789–795.
- Arch S (1972). Polypeptide secretion from the isolated parietovisceral ganglion of *Aplysia californica*. *J Gen Physiol* **59**, 47–59.
- Bae YS, Lee TG, Park JC, Hur JH, Kim Y, Heo K, Kwak JY, Suh PG & Ryu SH (2003). Identification of a compound that directly stimulates phospholipase C activity. *Mol Pharmacol* **63**, 1043–1050.
- Bandyopadhyay BC & Payne R (2004). Variants of TRP ion channel mRNA present in horseshoe crab ventral eye and brain. *J Neurochem* **91**, 825–835.
- Berridge MJ (2009). Inositol trisphosphate and calcium signalling mechanisms. *Biochim Biophys Acta* **1793**, 933–940.
- Berridge MJ & Irvine RF (1984). Inositol trisphosphate, a novel second messenger in cellular signal transduction. *Nature* **312**, 315–321.
- Berridge MJ & Irvine RF (1989). Inositol phosphates and cell signalling. *Nature* **341**, 197–205.
- Buehrer BM & Bell RM (1992). Inhibition of sphingosine kinase in vitro and in platelets. Implications for signal transduction pathways. *J Biol Chem* **267**, 3154–3159.
- Cantrell AR, Ma JY, Scheuer T & Catterall WA (1996). Muscarinic modulation of sodium current by activation of protein kinase C in rat hippocampal neurons. *Neuron* **16**, 1019–1026.
- Castagna M, Takai Y, Kaibuchi K, Sano K, Kikkawa U & Nishizuka Y (1982). Direct activation of calcium-activated, phospholipid-dependent protein kinase by tumor-promoting phorbol esters. *J Biol Chem* **257**, 7847–7851.
- Chakfe Y & Bourque CW (2000). Excitatory peptides and osmotic pressure modulate mechanosensitive cation channels in concert. *Nat Neurosci* **3**, 572–579.

- Chameau P, van de Vrede Y, Fossier P & Baux G (2001). Ryanodine-, IP₃- and NAADP-dependent calcium stores control acetylcholine release. *Pflugers Arch* **443**, 289–296.
- Conn PJ & Kaczmarek LK (1989). The bag cell neurons of *Aplysia*. A model for the study of the molecular mechanisms involved in the control of prolonged animal behaviours. *Mol Neurobiol* **3**, 237–273.
- Conn PJ, Strong JA, Azhderian EM, Nairn AC, Greengard P & Kaczmarek LK (1989a). Protein kinase inhibitors selectively block phorbol ester- or forskolin-induced changes in excitability of *Aplysia* neurons. *J Neurosci* **9**, 473–479.
- Conn PJ, Strong JA & Kaczmarek LK (1989b). Inhibitors of protein kinase C prevent enhancement of calcium current and action potentials in peptidergic neurons of *Aplysia*. *J Neurosci* **9**, 480–487.
- daCosta CJ, Ogrel AA, McCardy EA, Blanton MP & Baenziger JE (2002). Lipid-protein interactions at the nicotinic acetylcholine receptor. A functional coupling between nicotinic receptors and phosphatidic acid-containing lipid bilayers. *J Biol Chem* **277**, 201–208.
- Dargaei Z, Colmers PL, Hodgson HM & Magoski NS (2014). Electrical coupling between *Aplysia* bag cell neurons: characterization and role in synchronous firing. *J Neurophysiol* **112**, 2680–2696.
- Dargaei Z, Standage D, Groten CJ, Blohm G & Magoski NS (2015). Ca²⁺-induced uncoupling of *Aplysia* bag cell neurons. *J Neurophysiol* **113**, 808–821.
- Decrock E, De Bock M, Wang N, Gadicherla AK, Bol M, Delvaeye T, Vandenabeele P, Vinken M, Bultynck G, Krysko DV & Leybaert L (2013). IP₃, a small molecule with a powerful message. *Biochim Biophys Acta* **1833**, 1772–1786.
- DeRiemer SA, Greengard P & Kaczmarek LK (1985a). Calcium/phosphatidylserine/diacylglycerol-dependent protein phosphorylation in the *Aplysia* nervous system. *J Neurosci* **5**, 2672–2676.
- DeRiemer SA, Schweitzer B & Kaczmarek LK (1985b). Inhibitors of calcium-dependent enzymes prevent the onset of afterdischarge in the peptidergic bag cell neurons of *Aplysia*. *Brain Res* **340**, 175–180.
- DeRiemer SA, Strong JA, Albert KA, Greengard P & Kaczmarek LK (1985c). Enhancement of calcium current in *Aplysia* neurones by phorbol ester and protein kinase C. *Nature* **313**, 313–316.
- Dietrich A, Kalwa H, Rost BR & Gudermann T (2005). The diacylglycerol-sensitive TRPC3/6/7 subfamily of cation channels: Functional characterization and physiological relevance. *Pflugers Arch* **451**, 72–80.
- Doerner D, Pitler TA & Alger BE (1988). Protein kinase C activators block specific calcium and potassium current components in isolated hippocampal neurons. *J Neurosci* **8**, 4069–4078.
- Fink LA, Connor JA & Kaczmarek LK (1988). Inositol triphosphate releases intracellularly stored calcium and modulates ion channels in molluscan neurons. *J Neurosci* **8**, 2544–2555.
- Fisher SK, Novak JE & Agranoff BW (2002). Inositol and higher inositol phosphates in neural tissues: homeostasis, metabolism and functional significance. *J Neurochem* **82**, 736–754.
- Fisher T, Lin CH & Kaczmarek LK (1993). The peptide FMRFa terminates a discharge in *Aplysia* bag cell neurons by modulating calcium, potassium, and chloride conductances. *J Neurophysiol* **69**, 2164–2173.
- Fisher TE, Levy S & Kaczmarek LK (1994). Transient changes in intracellular calcium associated with a prolonged increase in excitability in neurons of *Aplysia californica*. *J Neurophysiol* **71**, 1254–1257.
- Franco A Jr & Lansman JB (1990). Stretch-sensitive channels in developing muscle cells from a mouse cell line. *J Physiol* **427**, 361–380.
- Fukami K, Inanobe S, Kanemaru K & Nakamura Y (2010). Phospholipase C is a key enzyme regulating intracellular calcium and modulating the phosphoinositide balance. *Prog Lipid Res* **49**, 429–437.
- Fulton D, Condro MC, Pearce K & Glanzman DL (2008). The potential role of postsynaptic phospholipase C activity in synaptic facilitation and behavioural sensitization in *Aplysia*. *J Neurophysiol* **100**, 108–116.
- Gardam KE, Geiger JE, Hickey CM, Hung AY & Magoski NS (2008). Flufenamic acid affects multiple currents and causes intracellular Ca²⁺ release in *Aplysia* bag cell neurons. *J Neurophysiol* **100**, 38–49.
- Gardam KE & Magoski NS (2009). Regulation of cation channel voltage and Ca²⁺ dependence by multiple modulators. *J Neurophysiol* **102**, 259–271.
- Geiger JE, Hickey CM & Magoski NS (2009). Ca²⁺ entry through a non-selective cation channel in *Aplysia* bag cell neurons. *Neuroscience* **162**, 1023–1038.
- Gogelein H, Dahlem D, Englert HC & Lang HJ (1990). Flufenamic acid, mefenamic acid and niflumic acid inhibit single nonselective cation channels in the rat exocrine pancreas. *FEBS Lett* **268**, 79–82.
- Gogelein H & Pfannmuller B (1989). The nonselective cation channel in the basolateral membrane of rat exocrine pancreas. Inhibition by 3',5'-dichlorodiphenylamine-2-carboxylic acid (DCDPC) and activation by stilbene disulfonates. *Pflugers Arch* **413**, 287–298.
- Grand T, Demion M, Norez C, Mettey Y, Launay P, Becq F, Bois P & Guinamard R (2008). 9-Phenanthrol inhibits human TRPM4 but not TRPM5 cationic channels. *Br J Pharmacol* **153**, 1697–1705.
- Green KA & Cottrell GA (1997). Modulation of ligand-gated dopamine channels in *Helix* neurones. *Pflugers Arch* **434**, 313–322.
- Groten CJ & Magoski NS (2015). PKC enhances the capacity for secretion by rapidly recruiting covert voltage-gated Ca²⁺ channels to the membrane. *J Neurosci* **35**, 2747–2765.
- Groten CJ, Rebane JT, Blohm G & Magoski NS (2013). Separate Ca²⁺ sources are buffered by distinct Ca²⁺ handling systems in *Aplysia* neuroendocrine cells. *J Neurosci* **33**, 6476–6491.
- Gryniewicz G, Poenie M & Tsien RY (1985). A new generation of Ca²⁺ indicators with greatly improved fluorescence properties. *J Biol Chem* **260**, 3440–3450.
- Guinamard R, Hof T & Del Negro CA (2014). The TRPM4 channel inhibitor 9-phenanthrol. *Br J Pharmacol* **171**, 1600–1613.

- Haj-Dahmane S & Andrade R (1997). Calcium-activated cation nonselective current contributes to the fast afterdepolarization in rat prefrontal cortex neurons. *J Neurophysiol* **78**, 1983–1989.
- Hamill OP, Marty A, Neher E, Sakmann B & Sigworth FJ (1981). Improved patch-clamp techniques for high-resolution current recording from cells and cell-free membrane patches. *Pflugers Arch* **391**, 85–100.
- Hannun YA, Loomis CR, Merrill AH Jr & Bell RM (1986). Sphingosine inhibition of protein kinase C activity and of phorbol dibutyrate binding in vitro and in human platelets. *J Biol Chem* **261**, 12604–12609.
- Helliwell RM & Large WA (1997). α_1 -Adrenoceptor activation of a non-selective cation current in rabbit portal vein by 1,2-diacyl-*sn*-glycerol. *J Physiol* **499**, 417–428.
- Hickey CM, Geiger JE, Groten CJ & Magoski NS (2010). Mitochondrial Ca^{2+} activates a cation current in *Aplysia* bag cell neurons. *J Neurophysiol* **103**, 1543–1556.
- Hickey CM, Groten CJ, Sham L, Carter CJ & Magoski NS (2013). Voltage-gated Ca^{2+} influx and mitochondrial Ca^{2+} initiate secretion from *Aplysia* neuroendocrine cells. *Neuroscience* **250**, 755–772.
- Hidaka H, Inagaki M, Kawamoto S & Sasaki Y (1984). Isoquinolinesulfonamides, novel and potent inhibitors of cyclic nucleotide dependent protein kinase and protein kinase C. *Biochemistry* **23**, 5036–5041.
- Hofmann T, Chubunov V, Gudermann T & Montell C (2003). TRPM5 is a voltage-modulated and Ca^{2+} -activated monovalent selective cation channel. *Curr Biol* **13**, 1153–1158.
- Hofmann T, Obukhov AG, Schaefer M, Harteneck C, Gudermann T & Schultz G (1999). Direct activation of human TRPC6 and TRPC3 channels by diacylglycerol. *Nature* **397**, 259–263.
- Hung AY & Magoski NS (2007). Activity-dependent initiation of a prolonged depolarization in *Aplysia* bag cell neurons: role for a cation channel. *J Neurophysiol* **97**, 2465–2479.
- Jin I & Hawkins RD (2003). Presynaptic and postsynaptic mechanisms of a novel form of homosynaptic potentiation at *Aplysia* sensory-motor neuron synapses. *J Neurosci* **23**, 7288–7297.
- Ju M, Shi J, Saleh SN, Albert AP & Large WA (2010). $\text{Ins}(1,4,5)\text{P}_3$ interacts with PIP_2 to regulate activation of TRPC6/C7 channels by diacylglycerol in native vascular myocytes. *J Physiol* **588**, 1419–1433.
- Kaczmarek LK (1986). Phorbol esters, protein phosphorylation and the regulation of neuronal ion channels. *J Exp Biol* **124**, 375–392.
- Kehoe J (1972). Three acetylcholine receptors in *Aplysia* neurones. *J Physiol* **225**, 115–146.
- Kim SJ, Kim YS, Yuan JP, Petralia RS, Worley PF & Linden DJ (2003). Activation of the TRPC1 cation channel by metabotropic glutamate receptor mGluR1. *Nature* **426**, 285–291.
- Kim Y, Yan AC, Power JM, Tadros SF, Klugmann M, Moorhouse AJ, Bertrand PP & Housley GD (2012). Alternative splicing of the TRPC3 ion channel calmodulin/ IP_3 receptor-binding domain in the hindbrain enhances cation flux. *J Neurosci* **32**, 11414–11423.
- Kishimoto A, Takai Y, Mori T, Kikkawa U & Nishizuka Y (1980). Activation of calcium and phospholipid-dependent protein kinase by diacylglycerol, its possible relation to phosphatidylinositol turnover. *J Biol Chem* **255**, 2273–2276.
- Kupfermann I & Kandel ER (1970). Electrophysiological properties and functional interconnections of two symmetrical neurosecretory clusters (bag cells) in abdominal ganglion of *Aplysia*. *J Neurophysiol* **33**, 865–876.
- Launay P, Fleig A, Perraud AL, Scharenberg AM, Penner R & Kinet JP (2002). TRPM4 is a Ca^{2+} -activated nonselective cation channel mediating cell membrane depolarization. *Cell* **109**, 397–407.
- Li HS, Xu XZ & Montell C (1999). Activation of a TRPC3-dependent cation current through the neurotrophin BDNF. *Neuron* **24**, 261–273.
- Liu D & Liman ER (2003). Intracellular Ca^{2+} and the phospholipid PIP_2 regulate the taste transduction ion channel TRPM5. *Proc Natl Acad Sci U S A* **100**, 15160–15165.
- Loechner KJ, Azhderian EM, Dreyer R & Kaczmarek LK (1990). Progressive potentiation of peptide release during a neuronal discharge. *J Neurophysiol* **63**, 738–744.
- Loechner KJ, Mattessich-Arrandale J, Azhderian EM & Kaczmarek LK (1992). Inhibition of peptide release from invertebrate neurons by the protein kinase inhibitor H-7. *Brain Res* **581**, 315–318.
- Lupinsky DA & Magoski NS (2006). Ca^{2+} -dependent regulation of a non-selective cation channel from *Aplysia* bag cell neurones. *J Physiol* **575**, 491–506.
- Magoski NS & Kaczmarek LK (2005). Association/dissociation of a channel-kinase complex underlies state-dependent modulation. *J Neurosci* **25**, 8037–8047.
- Michel S & Wayne NL (2002). Neurohormone secretion persists after post-afterdischarge membrane depolarization and cytosolic calcium elevation in peptidergic neurons in intact nervous tissue. *J Neurosci* **22**, 9063–9069.
- Michell RH (1975). Inositol phospholipids and cell surface receptor function. *Biochim Biophys Acta* **415**, 81–147.
- Nakhost A, Forscher P & Sossin WS (1998). Binding of protein kinase C isoforms to actin in *Aplysia*. *J Neurochem* **71**, 1221–1231.
- Nishizuka Y (1984). The role of protein kinase C in cell surface signal transduction and tumour promotion. *Nature* **308**, 693–698.
- Nishizuka Y (1988). The molecular heterogeneity of protein kinase C and its implications for cellular regulation. *Nature* **334**, 661–665.
- Okada T, Inoue R, Yamazaki K, Maeda A, Kurosaki T, Yamakuni T, Tanaka I, Shimizu S, Ikenaka K, Imoto K & Mori Y (1999). Molecular and functional characterization of a novel mouse transient receptor potential protein homologue TRP7. Ca^{2+} -permeable cation channel that is constitutively activated and enhanced by stimulation of G protein-coupled receptor. *J Biol Chem* **274**, 27359–27370.
- Partridge LD & Valenzuela CF (2000). Block of hippocampal CAN channels by flufenamate. *Brain Res* **867**, 143–148.
- Perney TM & Kaczmarek LK (1992). The role of inositol phosphates in neuronal function. *Adv Second Messenger Phosphoprotein Res* **26**, 311–333.

- Piomelli D, Shapiro E, Feinmark SJ & Schwartz JH (1987a). Metabolites of arachidonic acid in the nervous system of *Aplysia*: possible mediators of synaptic modulation. *J Neurosci* **7**, 3675–3686.
- Piomelli D, Volterra A, Dale N, Siegelbaum SA, Kandel ER, Schwartz JH & Belardetti F (1987b). Lipoxygenase metabolites of arachidonic acid as second messengers for presynaptic inhibition of *Aplysia* sensory cells. *Nature* **328**, 38–43.
- Popp R, Englert HC, Lang HJ & Gogelein H (1993). Inhibitors of nonselective cation channels in cells of the blood-brain barrier. *EXS* **66**, 213–218.
- Rane SG & Dunlap K (1986). Kinase C activator 1,2-oleoylacetyl glycerol attenuates voltage-dependent calcium current in sensory neurons. *Proc Natl Acad Sci USA* **83**, 184–188.
- Rhee SG (2001). Regulation of phosphoinositide-specific phospholipase C. *Annu Rev Biochem* **70**, 281–312.
- Savolainen K, Hirvonen MR & Naarala J (1994). Phosphoinositide second messengers in cholinergic excitotoxicity. *Neurotoxicology* **15**, 493–502.
- Sawada M, Cleary LJ & Byrne JH (1989). Inositol trisphosphate and activators of protein kinase C modulate membrane currents in tail motor neurons of *Aplysia*. *J Neurophysiol* **61**, 302–310.
- Shaw T, Lee RJ & Partridge LD (1995). Action of diphenylamine carboxylate derivatives, a family of non-steroidal anti-inflammatory drugs, on $[Ca^{2+}]_i$ and Ca^{2+} -activated channels in neurons. *Neurosci Lett* **190**, 121–124.
- Sossin WS, az-Arrastia R & Schwartz JH (1993). Characterization of two isoforms of protein kinase C in the nervous system of *Aplysia californica*. *J Biol Chem* **268**, 5763–5768.
- Sossin WS, Fan X & Saberi F (1996). Expression and characterization of *Aplysia* protein kinase C: a negative regulatory role for the E region. *J Neurosci* **16**, 10–18.
- Strong JA, Fink L, Fox A & Kaczmarek LK (1987a). Multiple roles for calcium and calcium-dependent enzymes in the activation of peptidergic neurons of *Aplysia*. *Soc Gen Physiol Ser* **42**, 187–199.
- Strong JA, Fox AP, Tsien RW & Kaczmarek LK (1987b). Stimulation of protein kinase C recruits covert calcium channels in *Aplysia* bag cell neurons. *Nature* **325**, 714–717.
- Sturgeon RM & Baenziger JE (2010). Cations mediate interactions between the nicotinic acetylcholine receptor and anionic lipids. *Biophys J* **98**, 989–998.
- Takai Y, Kishimoto A, Kikkawa U, Mori T & Nishizuka Y (1979). Unsaturated diacylglycerol as a possible messenger for the activation of calcium-activated, phospholipid-dependent protein kinase system. *Biochem Biophys Res Commun* **91**, 1218–1224.
- Tam AK, Gardam KE, Lamb S, Kachoei BA & Magoski NS (2011). Role for protein kinase C in controlling *Aplysia* bag cell neuron excitability. *Neuroscience* **179**, 41–55.
- Tam AK, Geiger JE, Hung AY, Groten CJ & Magoski NS (2009). Persistent Ca^{2+} current contributes to a prolonged depolarization in *Aplysia* bag cell neurons. *J Neurophysiol* **102**, 3753–3765.
- Toullec D, Pianetti P, Coste H, Bellevergue P, Grand-Perret T, Ajakane M, Baudet V, Boissin P, Boursier E, Loriolle F, Duhamell L, Charon D & Kirilovsky J (1991). The bisindolylmaleimide GF 109203X is a potent and selective inhibitor of protein kinase C. *J Biol Chem* **266**, 15771–15781.
- Tu P, Kunert-Keil C, Lucke S, Brinkmeier H & Bouron A (2009). Diacylglycerol analogues activate second messenger-operated calcium channels exhibiting TRPC-like properties in cortical neurons. *J Neurochem* **108**, 126–138.
- Venkatachalam K, Zheng F & Gill DL (2003). Regulation of canonical transient receptor potential (TRPC) channel function by diacylglycerol and protein kinase C. *J Biol Chem* **278**, 29031–29040.
- Villareal G, Li Q, Cai D, Fink AE, Lim T, Bougie JK, Sossin WS & Glanzman DL (2009). Role of protein kinase C in the induction and maintenance of serotonin-dependent enhancement of the glutamate response in isolated siphon motor neurons of *Aplysia californica*. *J Neurosci* **29**, 5100–5107.
- Vorndran C, Minta A & Poenie M (1995). New fluorescent calcium indicators designed for cytosolic retention or measuring calcium near membranes. *Biophys J* **69**, 2112–2124.
- White SH, Carter CJ & Magoski NS (2014). A potentially novel nicotinic receptor in *Aplysia* neuroendocrine cells. *J Neurophysiol* **112**, 446–462.
- White SH & Magoski NS (2012). Acetylcholine-evoked afterdischarge in *Aplysia* bag cell neurons. *J Neurophysiol* **107**, 2672–2685.
- Wilson GF, Magoski NS & Kaczmarek LK (1998). Modulation of a calcium-sensitive nonspecific cation channel by closely associated protein kinase and phosphatase activities. *Proc Natl Acad Sci U S A* **95**, 10938–10943.
- Yang XC & Sachs F (1989). Block of stretch-activated ion channels in *Xenopus* oocytes by gadolinium and calcium ions. *Science* **243**, 1068–1071.
- Zhang XF, Hyland C, Van GD & Forscher P (2012). Calcineurin-dependent cofilin activation and increased retrograde actin flow drive 5-HT-dependent neurite outgrowth in *Aplysia* bag cell neurons. *Mol Biol Cell* **23**, 4833–4848.
- Zhang Y, Helm JS, Senatore A, Spafford JD, Kaczmarek LK & Jonas EA (2008). PKC-induced intracellular trafficking of Ca_v2 precedes its rapid recruitment to the plasma membrane. *J Neurosci* **28**, 2601–2612.
- Zhang Y, Magoski NS & Kaczmarek LK (2002). Prolonged activation of Ca^{2+} -activated K^+ current contributes to the long-lasting refractory period of *Aplysia* bag cell neurons. *J Neurosci* **22**, 10134–10141.

Additional information

Competing interests

None declared.

Author contributions

R.M.S. conducted experiments and analysed data. R.M.S. and N.S.M. conceived and designed the project. R.M.S. wrote the manuscript. N.S.M. revised the manuscript. Both authors have approved the final version of the manuscript and agree to be accountable for all aspects of the work. All persons designated as authors qualify for authorship, and all those who qualify for authorship are listed.

Funding

This work was supported by a Canadian Institutes of Health Research grant (MOP111211) to N.S.M. R.M.S. holds an Ontario Graduate Scholarship, Doctoral.

Acknowledgements

The authors thank H. M. Hodgson and C. A. London for technical assistance.